NIKHEF

NATIONAAL INSTITUUT VOOR KERNFYSICA EN HOGE-ENERGIEFYSICA

受入
87-9-472
高工研図書室

1987

NIKHEF-H/87-8

HIGH RESOLUTION HADRON CALORIMETRY

Richard Wigmans
NIKHEF-H, Amsterdam, The Netherlands

ABSTRACT

The components that contribute to the signal of a hadron calorimeter and the factors that affect its performance are discussed, concentrating on two aspects: energy resolution and signal linearity. Both are decisively dependent on the relative response to the electromagnetic and the non-electromagnetic shower components, the e/h signal ratio, which should be equal to 1.0 for optimal performance. The factors that determine the value of this ratio are examined. The calorimeter performance is crucially determined by its response to the abundantly present soft neutrons in the shower. The presence of a considerable fraction of hydrogen atoms in the active medium is essential for achieving the best possible results. Firstly, this allows one to tune e/h to the desired value by choosing the appropriate sampling fraction. And secondly, the efficient neutron detection via recoil protons in the read-out medium itself reduces considerably the effect of fluctuations in binding energy losses at the nuclear level, which dominate the intrinsic energy resolution. Signal equalization, or compensation ($e/h = 1.0$) does not seem to be a property unique to ^{238}U, but can also be achieved with lead and probably even iron absorbers.

Invited talk given at the International Conference on Advances in Experimental Methods for Colliding Beam Physics, SLAC, March 9-13, 1987

HIGH RESOLUTION HADRON CALORIMETRY

Richard Wigmans
NIKHEF-H, Amsterdam, The Netherlands

ABSTRACT

The components that contribute to the signal of a hadron calorimeter and the factors that affect its performance are discussed, concentrating on two aspects: energy resolution and signal linearity. Both are decisively dependent on the relative response to the electromagnetic and the non-electromagnetic shower components, the e/h signal ratio, which should be equal to 1.0 for optimal performance. The factors that determine the value of this ratio are examined. The calorimeter performance is crucially determined by its response to the abundantly present soft neutrons in the shower. The presence of a considerable fraction of hydrogen atoms in the active medium is essential for achieving the best possible results. Firstly, this allows one to tune e/h to the desired value by choosing the appropriate sampling fraction. And secondly, the efficient neutron detection via recoil protons in the readout medium itself reduces considerably the effect of fluctuations in binding energy losses at the nuclear level, which dominate the intrinsic energy resolution. Signal equalization, or compensation ($e/h = 1.0$) does not seem to be a property unique to ^{238}U, but can also be achieved with lead and probably even iron absorbers.

Invited talk given at the International Conference on Advances
in Experimental Methods for Colliding Beam Physics
SLAC, March 9 - 13, 1987

1. INTRODUCTION

Large hadron calorimeters will be crucial components in any experiment at future high energy colliding beam machines. Calorimeters offer unique possibilities to recognize rare events at the trigger level, and to measure the characteristics of these selected events under severe background conditions, with a compact instrument. Achieving the best possible energy resolution is closely linked to the capability of detecting new phenomena in high energy physics. The energy resolution determines, for example, the mass resolution for detecting new particles that decay into jets (Higgs), the limits on missing (transverse) energy that can be handled (SUSY particle production), and the kinematic range accessible for data analysis (ep scattering). In order to be able to design calorimeters optimally it is, therefore, of vital interest to understand the factors that limit the energy resolution in as much detail as possible.

Calorimeters for the detection of electromagnetically interacting particles (e,γ) are well understood and can be reliably simulated in great detail by Monte-Carlo techniques (e.g. EGS4). This is by no means the case for hadron calorimeters. To date there exists no computer program that is capable of simulating the complete development of a hadronic cascade and predicting reliably the response of a given calorimeter to it. As a consequence, progress in this area of detector technology had to proceed on a trial-and-error basis for a long time. Many results obtained in this process were considered extremely confusing.

The crucial role of the so-called e/h signal ratio for the energy resolution was already recognized in the early days of hadron calorimetry[1] . The R807 group at CERN demonstrated that energy resolutions of $35\%/\sqrt{E}$ could be achieved for hadron detection with their uranium/plastic-scintillator sandwich calorimeter, which had an e/h ratio close to the desired value 1.0[2] . Measurements performed by HELIOS recently showed that the energy resolution of this detector scales with $E^{-\frac{1}{2}}$ up to the TeV regime, and that deviations from signal linearity are negligible over 3 orders of magnitude in energy[3] .

Measurements performed with non-compensating ($e/h \neq 1$) devices, however,

showed considerable deviations from linearity, and energy resolutions σ/E that do not improve as $E^{-\frac{1}{2}}$ with increasing energy[4] . The constant term that has to be introduced in order to describe the energy resolution is typically 5 % and, therefore, dominates the result at energies beyond 100 GeV, where the new physics has to be found.

However, the use of ^{238}U as absorber material is by no means a guarantee for superior performance. Prototype tests by SLD and D0, using liquid argon readout, gave disappointing results, to the extent that SLD even abandoned the idea of using uranium and switched to a lead absorber that gave results of similar quality. Also the combination uranium/plastic-scintillator turned out not to be magic: WA78 found overcompensation ($e/h \approx 0.8$) and rather poor energy resolutions[5] . On the other hand Brückmann *et al.* from the ZEUS Collaboration, who basically copied the HELIOS design for their prototype studies, found equally good performance[6] .

Recently, understanding of hadron calorimetry has considerably improved. We systematically investigated in detail the response of a sampling calorimeter to the various components of a hadron shower[7] . It turned out that the calorimeter performance in terms of energy resolution and signal linearity is crucially determined by its response to the abundantly present soft neutrons in the shower. The presence of a considerable fraction of hydrogen atoms in the readout medium is essential for the best possible performance. Firstly, this allows one to tune e/h to the desired value (1.0) by choosing the appropriate sampling fraction. And secondly, the efficient neutron detection via recoil protons in the readout medium itself reduces considerably the effect of fluctuations in binding energy losses at the nuclear level, which dominate the intrinsic energy resolution. The confusing experimental results mentioned before were quite nicely reproduced in this study.

In this paper, the theoretical framework that lead to this improved understanding is briefly described. In section 2, we will discuss how the e/h value affects the calorimeter performance. In section 3, we describe how the properties of the passive and active calorimeter materials determine its e/h value. In section 4, the factors that determine the energy resolution of practical calorimeters are examined. An outlook is given in

section 5. Since this paper has to be necessarily brief, only a rather global description can be given. For details the reader is referred to the original work[7] .

2. EFFECTS OF THE e/h RATIO ON THE CALORIMETER PERFORMANCE

Since calorimetry is based on statistical processes, the measurement accuracy increases with energy, contrary to tracking detectors based on momentum analysis in a magnetic field. This is a very attractive feature. When a particle develops a shower in a block of matter that we call a sampling calorimeter, some fraction of its energy is transformed into a measurable signal, usually a pulse of electrical charge. This pulse is the result of all the charged particles generated in the shower development, that traverse and ionise the active layers of the detector. The energy resolution for detecting the original particle is determined by the fluctuations occurring in this process, which affect the size of the resulting signal. Amongst these we mention

a) Sampling fluctuations, due to the fact that only a (small) fraction of the energy is deposited in the active layers and, therefore, contributes to the calorimeter signal. It has been shown[8] that if this fraction is larger than $\sim 1\%$, the effect is dominated by fluctuations in the total number of gap crossings by charged particles generated in the shower. Therefore, the contribution of this source of fluctuations is, to first order, for a given absorber material proportional to the square root of the thickness of the absorber plates, and insensitive to the type and thickness of the active layers. The latter part of this statement is not correct if the active layers are so thin (expressed in g/cm^2), that the statistical fluctuations in the number of ionization processes per gap crossing become important. This is for example the case for gaseous media, where Landau and path length fluctuations dominate those mentioned before. In *electromagnetic* sampling calorimeters, sampling fluctuations are the major contribution to the energy resolution.

b) Fluctuations in the fraction of the energy deposited in the form of ionizing parti-

cles. These effects usually dominate the energy resolution of *hadron* calorimeters. An obvious component comes from incomplete shower containment, *i.e.* from secondary particles like $\mu, \nu, \mathrm{n}, \mathrm{K}_{\mathrm{L}}^{0}$, etc. that (partly) escape detection. A somewhat less obvious, but usually far more important source of fluctuations comes from the energy losses at the nuclear level. The energy needed to release the nucleons and nucleon aggregates like α-particles that are bound in atomic nuclei, is lost for detection. The fraction of the initial hadron energy spent in this way is considerable, up to $\sim$ 40% on average for the non-electromagnetic part of hadron showers in high-Z elements. Due to the enormous variety of possible nuclear interactions, the fluctuations about this number are a major contribution to the energy resolution of hadron calorimeters.

The latter class of effects has no equivalent in electromagnetic showers. This has consequences for calorimetric hadron detection. Firstly, the signal distribution for hadrons of energy E will be broader than for electromagnetic showers at the same energy, because of the larger fluctuations. Secondly, the average response (signal per unit of energy) will have a different value for electromagnetic and hadronic showers ($e/h \neq 1$). Because of the losses mentioned before, the latter will in general be smaller ($e/h > 1$).

In the development of a shower generated by a high-energy hadron some fraction ($\mathrm{f_{em}}$) of the energy is usually spent on the production of π^0's and η's. A hadron shower, therefore, has in general an electromagnetic (em) and a non-electromagnetic component. Because of the reasons just given, the calorimeter response to these components will be different (see fig. 1). The fluctuations in $\mathrm{f_{em}}$ are large and non-Gaussian. Moreover, $< \mathrm{f_{em}} >$ increases (logarithmically) with energy. If $e/h \neq 1$, this has the following consequences for the calorimeter performance:

i) The fluctuations in $\mathrm{f_{em}}$ give an additional contribution to the energy resolution.

ii) Because of the non-Gaussian nature of the fluctuations in $\mathrm{f_{em}}$ the energy resolution σ/E will not improve as $E^{-\frac{1}{2}}$ with increasing energy.

iii) The calorimeter signal is not proportional to the hadron energy (alinearity).

iv) The measured e/h signal ratio is energy dependent.

All these effects have been experimentally observed. This is illustrated by fig. 2 , which shows experimental data on calorimetric hadron detection with an iron/plastic-scintillator ($e/h \approx 1.4$) calorimeter[4] , and with uranium/plastic-scintillator[3] ($e/h = 1$). The energy resolution obtained with iron is much worse than for uranium and it does not scale as $E^{-\frac{1}{2}}$. The calorimeter response for iron rises with energy, and consequently the e/h signal ratio decreases as the energy is increased. Such effects are absent for uranium.

To avoid the confusion caused by the latter effect, we prefer to use the energy-independent quantity $e/h^{\rm intr}$, given by the ratio of the mean values of the two curves in fig. 1 . The relation between $e/h^{\rm intr}$ and e/h is given by

$$e/h(E) = \frac{e/h^{\rm intr}}{1 - < {\rm f_{em}}(E) > [1 - e/h^{\rm intr}]}$$

where

$$< {\rm f_{em}}(E) > = 0.1 \ln E({\rm GeV})$$

is a reasonable approximation in the energy range 10 - 100 GeV[9] . At 10 GeV, where e/h ratios are frequently given, the difference between the measured e/h value and $e/h^{\rm intr}$ is usually small, less than 10%.

We investigated the effects of $e/h \neq 1$ on the calorimeter performance with a very simple Monte Carlo simulation, making some reasonable assumptions on the widths of the distributions in fig. 1 , on $< {\rm f_{em}}(E) >$, and on the fluctuations in ${\rm f_{em}}(E)$. The results are given in fig. 3 , where curves for the energy resolution and the calorimeter response are plotted for various values of $e/h(10\,{\rm GeV})$. The data on the energy resolution are plotted using an abcissa linear in $E^{-\frac{1}{2}}$. This shows that the deviation from $E^{-\frac{1}{2}}$ scaling can be very reasonably described as a constant term, the value of which is determined by e/h. This figure makes it very clear that, in particular at high energies, the value of $e/h^{\rm intr}$ is crucial for the energy resolution that can be obtained. For the CDHS calorimeter ($e/h = 1.36$ at 10 GeV), the resolution σ/E does not become better than $\sim 7\%$, even at the highest energies. For calorimeters with $e/h^{\rm intr} = 1$, the energy resolution will continue to improve with increasing energy, until limitations due to instrumental effects

become important. HELIOS have experimentally shown that energy resolutions close to 1% are feasible for such devices[3] .

If $e/h = 1$, the contribution of fluctuations in f_{em} to the energy resolution are eliminated. It has been advocated that there are other ways to (partly) achieve this goal. The em and non-em shower components have very different characteristic dimensions, particularly in high-Z absorber materials. If the calorimeter is sufficiently finely segmented one might, therefore, determine f_{em} on an event-by-event basis and hence eliminate, at least partly, the effects of fluctuations in this number. The CDHS Collaboration developed an algorithm for this purpose, with which they were able to restore $E^{-\frac{1}{2}}$ scaling for the energy resolution of single pion detection in their very fine-grained detector (read out every 7 radiation lengths in depth)[4] . Unfortunately, alinearities of $\sim$ 10% remained after this procedure, which involved energy-dependent weighting factors (see fig. 2). This means that the procedure will probably not work (as well) for the detection of jets, where the showers generated by individual hadrons overlap, and where the number of jet particles and their energy is not a priori known. In any case, these methods have never been experimentally demonstrated to improve the resolution under such conditions.

Because of these reasons, we think that a calorimeter with $e/h^{\rm intr} = 1$ has essential advantages, which cannot be compensated for by a very fine-grained readout in case $e/h \neq 1$. We will now examine which factors determine the e/h signal ratio, and how this ratio is affected by the properties of the calorimeter materials.

3. THE CALORIMETER RESPONSE TO THE SHOWER COMPONENTS

3.1 The procedure of calculating e/h

In this section we will investigate the calorimeter response to the various components of a hadron shower. For a particular type of secondary particles, the signal will be determined by two factors:

i) The fraction of the energy used to ionise the active layers.

ii) The ionization density in these layers. Saturation effects may reduce the signal from densely ionizing particles, *e.g.* soft protons, considerably.

We distinguish the following classes of secondary particles:

a) High-energy photons and electrons from π^0 and η decay, that form the em shower component.

b) Ionizing hadrons (charged pions, kaons, protons, etc.).

c) Soft neutrons.

d) Soft γ's from nuclear deexcitation.

As a scale for the calorimeter signal, the response to a minimum-ionizing particle (mip) will be used. The fraction of the energy deposited by such a particle in the active layers of a given sampling calorimeter is called the sampling fraction $f_{\rm samp}$, and can be calculated immediately from the mean dE/dx value's for mip's in the calorimeter materials:

$$f_{\rm samp} = \frac{dE/dx[1\,\text{readout layer}]}{dE/dx[1\,\text{readout} + 1\,\text{absorber layer}]}$$

In practical calorimeters $f_{\rm samp}$ amounts to about $5-10\%$ for plastic scintillator or liquid argon (LAr) readout, $\sim 1\%$ for Si and $\sim 10^{-4}$ for wire chambers.

Relating the responses of the 4 mentioned types of particles to mip's, one can schematically write the e/h signal ratio as follows

$$e/h^{\rm intr} = \frac{e/mip}{f_{\rm ion}\, ion/mip + f_{\rm n}\, n/mip + f_\gamma\, \gamma/mip}$$

where $f_{\rm ion}$, $f_{\rm n}$ and f_γ are the average fractions of the energy in the non-em component, that are deposited in the form of ionizing hadrons, neutrons and nuclear γ's. We will now discuss the various terms of this expression.

3.2 The response to high-energy electron and photon showers (e/mip)

The signal from an em shower is the result of the ionization of the active layers by all the electrons and positrons generated in the shower development, which traverse these layers. Naïvely, one might therefore expect that this signal is equal to the one from muons traversing the detector, which lose an amount of energy $\Delta E = E_{\rm em}$. This is in practice usually not the case. Experimentally, one observes that in calorimeters with high-Z absorber material, the em signal is considerably suppressed with respect to mip's ($e/mip < 1$). If the Z-values of the active and passive media are about equal, like in Fe/LAr, e/mip is close to 1.

For historical reasons these phenomena are usually called transition effects, since it was assumed that they should be attributed to mechanisms affecting the shower composition at the boundary between layers of materials with different Z. This is not true.

The explanation of the transition effects is closely linked to the way in which soft γ's ($E_\gamma < 1\,\mathrm{MeV}$) that are generated in large numbers in an em shower, are absorbed in a mixture of materials. At these low energies, the photo-electric effect is an important mechanism. The cross section for this process is proportional to Z^5, while the ionization cross section for charged particles is to first order proportional to Z. In a calorimeter consisting of high-Z absorber material and low-Z active layers, the soft γ's will, therefore, almost exclusively interact with absorber atoms. Only if the interaction occurs sufficiently close to a boundary can the photo-electron produced in this process contribute to the measured signal. To illustrate this point, it can be mentioned that the mean range of a 1 (0.1) MeV electron in uranium is only 0.4 mm (20 microns). As a result, the calorimeter response to an em shower is suppressed with respect to mip's.

Analysis of shower simulation data from EGS4 clearly support this conclusion. Needless to say that for obtaining accurate results, the program should be run with cut-off values that are sufficiently low to correctly describe the peculiarities of the energy deposition by the soft shower component. Although we are dealing with very soft particles, the total amount of energy carried by them is considerable. The evolution of the computer

time needed for the simulation when lowering the cut-off values for E_γ and E_e, is already an indication for this. Figure 4 shows that in lead or uranium calorimeters $\sim 40\%$ of the total energy of a 10 GeV em shower is deposited through ionization by particles softer than 1 MeV, in which energy region the photo-electric effect is the dominating process.

For what concerns the response of high-Z sampling calorimeters, em showers consist of two rather well-separable components: The hard part (> 1 MeV), that can be reasonably described as a bunch of mip's, and the soft part (< 1 MeV) for which the detector is less efficient. This has some quite interesting consequences for (hadron) calorimetry, all of which are confirmed by EGS4 calculations:

a) The e/mip ratio changes with the depth of the shower, since the relative contribution of both components is a function of depth: The shower gets softer as the depth increases. In a longitudinally segmented calorimeter, calibrated with muons, the energy deposited by an electromagnetic shower in individual segments will be wrongly measured if the shower exceeds a segment boundary, although the *total* energy may be correct.

b) One can tune the e/mip, and hence the e/h value to a certain extent, since the relative contribution of the soft component to the calorimeter signal depends on the thickness of the absorber layers and also on the thickness of the active layers (see fig. 5). This can be understood as follows. Only photo-electrons produced close to a boundary contribute to the signal. If they manage to reach the active layers they are usually so soft that they do not penetrate very far. If either the absorber or the readout thickness is decreased, the "effective" boundary region becomes a larger fraction of the calorimeter as a whole and, therefore, the calorimeter response is increased. These effects are mainly important for very fine sampling.

c) In a high-Z calorimeter one may further reduce e/mip by inserting a low-Z foil in between the active and passive layers. This prevents photo-electrons produced in the high-Z material from reaching the active layers. This is illustrated in fig. 6, where the results of EGS4 calculations on a uranium/plastic-scintillator calorimeter are shown. The uranium plates are wrapped in stainless steel, the thickness of which

is varied. This wrapping decreases the "intrinsic" e/mip ratio by at maximum $\sim 8\%$ at 0.5 mm Fe. If the wrapping material is made thicker than that, interactions by the shower particles in iron will become more and more important, and tend to increase e/mip because $Z_{\mathrm{Fe}} \ll Z_{\mathrm{U}}$.

The detector inefficiency for the soft component of em showers in high-Z materials is an important ingredient for compensation, since it brings the em response closer to the non-em one. As we shall see later it is, however, not enough.

3.3 The response to nuclear gamma's (γ/mip)

In the non-em part of hadronic shower development large numbers of γ's are produced from nuclear deexcitation. Their energy spectrum depends on the characteristic nuclear level structure of the nuclides involved. In general, the vast majority of these γ's have an energy below 2 MeV.

In the previous subsection we saw that the transition effects observed for high-energy em showers are caused by the reduced detection efficiency for the soft γ shower component. The calorimeter signal suppression for nuclear γ's will, therefore, even be stronger than for these showers. This is confirmed by EGS4 calculations.

Since the mean photo-electron range is extremely energy-dependent, the detection efficiency decreases sharply below 1 MeV (fig. 7). At 0.511 MeV, the energy of the very abundant e^+ annihilation γ's, the signal is already reduced by a factor 7 compared to mip's, for the calorimeter in this example (HELIOS). The γ/mip signal ratio needed for the computation of e/h is sensitively dependent on the γ energy spectrum. For the measured spectrum of ^{238}U fission γ's, that was used throughout the calculations, we found γ/mip to be $\sim$ 0.4 in uranium calorimeters, versus 0.6 for e/mip. The EGS4 calculations showed that also the other effects found for em showers (figs. 5,6) were enhanced for a nuclear γ-ray spectrum.

Nuclear fission is an important source of nuclear γ's in uranium calorimeters. We measured that in the non-em part of hadron showers on average $\sim$ 10 fissions per GeV

are generated[10] . In each fission, on average 7.4 MeV is released in the form of prompt γ's[11] . Other processes like inelastic neutron scattering and thermal neutron capture further increase the fission-related nuclear γ component to a considerable fraction of the initial particle energy. The use of uranium absorber in hadron calorimeters was originally advocated because of this extra energy, which was assumed to make up for the inevitable losses in the non-em part of the shower (compensation)[12] . The reduced efficiency for detecting these γ's limits the effect of this, however, to the extent that the condition $e/h^{\rm intr} = 1$ can not be achieved in U/LAr calorimeters.

3.4 The non-em shower part ($f_{\rm ion}, f_{\rm n}, f_\gamma$)

The analysis of the calorimeter signal from em showers has taught us an important lesson, that is also relevant for understanding the details of the response to the non-em part. The lesson is, that the signal is decisively determined by the peculiarities of the processes occurring at the very last stages of the shower development. Although the energy is very low, the number of particles is so large that a considerable fraction of the total energy is deposited through these processes.

In the last stages of the development of the non-em shower part the production of pions, kaons, etc. is energetically impossible. It turns out that even at very high energies, the contribution of such particles to the calorimeter signal is small: Typically, only $10 - 15\%$ of the non-em energy is deposited through ionization by charged pions. An easy way to see this is by realizing that charged pions lose on average only ~ 0.2 GeV per nuclear interaction length through ionization of the medium that they traverse. A 100 GeV pion that produces in its first interaction 10 other charged pions will, therefore, have lost only $\sim 2\%$ of its energy when the secondary pions undergo strong interactions. The average pion multiplicity in these secondary interactions is probably something like 2 - 3 (adding another $4 - 6\%$ to the dE/dx loss). In further generations new pion production becomes rapidly negligible.

The remaining $85 - 90\%$ of the shower energy is spent on nuclear processes. It is used

to release nucleons and nucleon aggregates from atomic nuclei (binding energy losses), and to give kinetic energy to the reaction products. Usually the nuclei also emit γ's in these processes (see section 3.3). Apart from these γ's, protons and neutrons may contribute to the calorimeter signal. The range of the nucleon aggregates and of the recoiling target nuclei is so small that their kinetic energy is virtually lost for detection.

The way in which the protons and neutrons lose energy and contribute to the calorimeter signal is very different. The vast majority of the protons will lose their complete kinetic energy by ionization. Only the fast component ($E_{\rm kin} > 100\,{\rm MeV}$) may cause new nuclear reactions to occur at a non-negligible level. The neutrons *exclusively* lose kinetic energy through strong interactions. In these reactions new neutrons, protons and γ's may be produced, and additional binding energy lost. In particular the fast neutrons produced in the initial phase of the shower may develop quite complicated showers themselves.

The numerical details of the nuclear reaction mechanisms which are important for our purpose (*e.g.* nuclear spallation) are extensively discussed in ref. 7. Here we only give the main conclusions. The neutron multiplicity in hadron showers developing in a material ($Z \gg 1$) is much larger than the proton multiplicity, particularly if Z is large. This has two reasons:

a) More neutrons than protons are available in the target nuclei.

b) At low energies the nuclear Coulomb barrier will prevent protons from escaping.

In the reactions that start the "nuclear" phase of the shower development, more kinetic energy will therefore be carried away by neutrons than by protons. Most of this kinetic neutron energy will, however, be lost as nuclear binding energy in a series of subsequent reactions, in which the neutron multiplicity increases considerably, and in which also some new protons may be produced. In each nuclear reaction on average $2-3\,{\rm MeV}$ is released in the form of nuclear γ's.

At some stage in the shower development the neutrons have degraded so much in energy, that they cannot release any more new protons from target nuclei. For high-Z absorbers this is the case below $E_n^{\rm kin} \approx 20\,{\rm MeV}$. What we need to know at this

point in order to be able to compute $e/h^{\rm intr}$ (see sect. 3.1) are the fraction of the non-em energy deposited through ionization by protons (the major component of $f_{\rm ion}$), the remaining kinetic neutron energy ($f_{\rm n}$), and the total number of nuclear reactions (needed for f_γ). Nuclear γ's have only eaten up $2-3\%$ of the energy at this stage. The other components depend obviously on the Z of the absorber material. Roughly one may say that $f_{\rm ion} \approx Z/A$, while $f_{\rm n}$ varies from 8% for Fe to 15% for ^{238}U. The rest of the energy is invisible (binding energy, target recoil, nucleon aggregates). The contribution of nuclear fission in uranium becomes mainly important beyond this point in the shower development, *i.e.* for $E_n < 20\,\mathrm{MeV}$, because that is where the neutron multiplication and the energy gain from this process count most.

3.5 The response to ionizing hadrons (ion/mip)

As was shown in the previous subsection, this shower component is dominated by protons ($70-75\%$). The remaining contribution comes from pions, kaons, etc. These were considered mip's. The calorimeter signal ratio p/mip may deviate from 1 because of the following reasons:

i) The range of the spallation protons is limited (3 mm in U at 40 MeV). Sampling inefficiencies for the soft part of the spectrum *decrease* the p/mip value.

ii) The sampling fraction (see sect. 3.1) for non-relativistic particles may be very different from the mip value. The magnitude of this effect is very energy- and Z-dependent. Especially for high-Z absorbers p/mip may considerably *increase*.

iii) Saturation or recombination effects in the readout material *reduce* the response for densely ionizing particles, and hence the p/mip value.

iv) Multiple scattering of very soft protons *decreases* p/mip if $Z_{\rm abs} \gg Z_{\rm readout}$.

The combined effect of all these phenomena was investigated with a Monte-Carlo program. The ion/mip signal ratio turned out to depend on the material combination, on the proton energy spectrum, on the saturation properties of the readout material,

and on the thickness of the active layers. The first three effects are obvious from $i - iv$, the last effect is presumably due to the fact that if the thickness of the active layers is increased, a larger fraction of the protons will stop inside them and hence produce a relatively small signal compared to the amount of energy deposited (saturation).

An example of the results is given in fig. 8. This figure illustrates the energy dependence and the saturation effects. For practical calorimeters with saturating readout materials (plastic scintillator, LAr), *ion/mip* signal ratios were found in the range 0.85 – 1.0. For a non-saturating medium like Si the response would be $\sim 15\%$ larger.

3.6 The response to soft neutrons (n/mip)

Soft neutrons are the most interesting shower component, and the most crucial one for the calorimeter response. In the previous subsections we saw that the calorimeter response to the other shower components depends on rather global material properties, like $Z_{\rm abs}$. In order to be able to properly evaluate the neutron contribution, we have to go rather deeply into nuclear physics details. Nuclear level structures and cross sections for individual reactions are important for the result.

For example, the fact that the first excited state in the "double magic" nucleus ^{208}Pb lies as high as 2.6 MeV above the ground state level (which prevents inelastic neutron scattering below this energy), makes that the e/h ratio for a Pb/plastic-scintillator calorimeter would change considerably if the isotopes ^{204}Pb , ^{206}Pb , and ^{207}Pb , which can be excited by neutrons down to 0.6 MeV, would not be present. Small impurities with anomalously large cross sections for certain neutron-induced reactions, like Cd, may also have a large impact.

Fortunately, neutron scattering is one of the most systematically studied areas in physics. The wealth of existing experimental information allows to calculate rather precisely how the neutrons will lose their kinetic energy in a given calorimeter. Figure 9 shows cross sections, which are relevant for the calculations of neutron transport in a uranium/plastic-scintillator calorimeter. Proton production off uranium nuclei does

no longer occur at these low neutron energies. However, the neutrons can still multiply themselves, through $(n,2n)$ or $(n,3n)$ reactions where additional binding energy is lost, or through nuclear fission. The latter process may occur down to $E_n^{\rm kin} \approx 1.5\,{\rm MeV}$. In inelastic scattering kinetic neutron energy is converted into γ's, but also the probability for this process sharply decreases below 2 MeV.

The last step in the neutron's lifetime as a free particle is capture. In this proces, the energy that was needed to liberate the neutron from the nuclear field, is gained back and emitted by the capturing nucleus in the form of γ's. The cross section for this process is only considerable when the neutron is practically thermalized. The dominating process to get rid of the last $1-2\,{\rm MeV}$ is elastic scattering. The cross section for this process is very large, more than 4 b (mean free neutron path less than 5 cm). However, the energy loss per collision is very small, 1/239 on average. The reaction products, recoiling target nuclei, are undetectable.

The situation changes completely if the calorimeter also contains hydrogen, in the readout material. Hydrogen is well-known to be very efficient in thermalizing neutrons. In each elastic collision, on average half of the kinetic neutron energy is transferred. At 1 MeV the cross section for this process is 4 b, which corresponds to a mean free neutron path of ~ 5 cm in polystyrene, and ~ 4 cm in TMP. The reaction products of this process are recoil protons. These are produced inside the active layers, and contribute *directly* to the calorimeter signal, *i.e.* they are not sampled like mip's. The range of 1 MeV protons in polystyrene is 22 μm and, therefore, in practice the kinetic energy of protons produced in this way will almost *completely* be deposited in the active calorimeter layers.

In calorimeters that contain hydrogen atoms, neutron-proton scattering is a very important source of energy loss, because at low energies there is almost no competition from other processes. This may be concluded from an experimental study on the distribution of radioactive nuclides produced by the neutrons from hadron showers[10] . Figure 10 shows the longitudinal distributions of ^{239}Np, produced from thermal neutron capture by ^{238}U, in different uranium calorimeter configurations. It turned out that the distribution in uranium/plastic-scintillator is very different from the ones in uranium

calorimeters not containing hydrogen. The neutrons were much faster thermalized in the scintillator case and, therefore, must have lost a considerable fraction of their kinetic energy in elastic collisions with hydrogen nuclei. The reduced number of fissions measured in the scintillator calorimeter supports this conclusion as well.

We studied the transport of the soft neutron shower component in a given calorimeter structure with a Monte-Carlo program, that contained all the relevant information on the nuclear physics: The cross sections for all possible reactions in the absorber and readout materials, the energy transfer in these reactions, the physics on fission neutrons and γ's, etc. Since the recoil protons are very densely ionizing, the saturation characteristics of the readout materials are of crucial importance. We used Birk's law to convert from energy to signal (L):

$$L/E = [\int_0^{x_{max}} (1 + kB\frac{dE}{dx})dx]^{-1}$$

The values of the saturation constant kB are such that this meant a reduction of a factor $4 - 5$ for materials like LAr and plastic scintillator. Essential for the results was also the input neutron spectrum. We used a linear combination of two Maxwell distributions to account for the soft evaporation and fission neutrons on the one hand, and for the degraded spallation neutrons on the other hand. The validity of these assumptions was checked and found in excellent agreement with all the experimental data from the neutron-induced activation analysis mentioned before[10] .

Figure 11 shows an example of the results, for a 3 mm U/3 mm plastic-scintillator calorimeter. Below 4 MeV, more than half of the kinetic neutron energy is converted into recoil protons, and below 1 MeV even more than 70%. The remaining part of the energy is converted into γ's (inelastic scattering, fission) and invisible forms (binding energy, target recoil). Note that the sampling fraction, *i.e.* the part of the energy that mip's deposit in the active layers, amounts to only $\sim$ 10% for this calorimeter. The recoil protons will therefore substantially contribute to the calorimeter signal.

A nice example to illustrate this comes from the L3 Collaboration, who tested uranium calorimeters with proportional wire chamber readout[13] . When using isobutane

(containing hydrogen) the hadronic response was found to be about twice as high as for Ar/CO_2 (no hydrogen), while the electron response was almost gas-independent (see fig. 12). The difference is due to $n-p$ scattering. Similar differences occur between plastic-scintillator (containing hydrogen) and LAr (no hydrogen) readout. These are smaller than for gaseous media because of saturation effects, but yet considerable.

The Monte-Carlo studies revealed another very interesting effect. It turned out that the n/mip signal ratio, or the relative contribution of recoil protons to the calorimeter signal, is sensitively dependent on the sampling fraction for mip's (f_{samp} , see sect. 3.1). If f_{samp} gets smaller, n/mip increases; if f_{samp} gets larger, n/mip decreases. This can be understood as follows.

If the thickness of the absorber plates is increased, the signal from mip's will decrease proportionally. The energy transferred to recoil protons in the active layers by the neutrons is *not* sampled. We saw before that at low neutron energies, there is almost no alternative for this process and, therefore, the fraction of the neutron energy deposited in this form decreases much slower than the mip signal. In other words, if the sampling fraction is decreased, the n/mip signal ratio and hence the total non-em calorimeter response increases, and the e/h signal ratio decreases. The sampling fraction is, therefore, a crucial parameter for the performance of hadron calorimeters with hydrogenous readout.

Figure 13 shows some results of the calculations, for uranium/plastic-scintillator calorimeters. Instead of the sampling fraction, we used the more practical variable R_d, defined as the ratio of the thicknesses (in mm) of the passive and active calorimeter layers; R_d is approximately inversely proportional to f_{samp}. In fig. 13a the n/mip signal ratio is given as a function of R_d. The neutron signal is split up in its various contributing components. The dominating recoil proton contribution strongly increases with R_d. The consequences of this for the calorimeter performance are of decisive importance, because of the relatively large contribution of the soft-neutron shower component to the calorimeter signal. In the case of the compensating HELIOS calorimeter[2,3] ($R_d = 1.2$), these neutrons contribute almost 40% to the total non-em part of the signal, and for the

overcompensating WA78 detector[5] ($R_d = 2 - 3$) even 50%.

Figure 13a also shows that the neutrons do not only contribute to the calorimeter signal through recoil protons, but also through the γ's that they produce by fission, inelastic scattering and capture. This contribution is limited because of the small γ/mip signal ratio (sect. 3.3). Nevertheless, a considerable fraction of the energy is deposited in this form, in particular through the neutron capture process. We measured that in uranium $\sim$ 50 neutrons/GeV are produced in the non-em shower part[10] . If these are all captured, 240 MeV/GeV is released as capture γ's. Their contribution to the calorimeter signal depends on the capture cross section, on the calorimeter size and, since thermalization is a slow process, on the signal integration time.

Figure 13b shows the sensitivity of the e/h signal ratio to the fraction of the neutrons that contribute to the signal through capture ($f_{\rm capt}$). Calculations by Brückmann[14] indicate that in 100 ns, a typical gate time for scintillator readout, $f_{\rm capt} \approx 20\%$. Measurements on the evolution of the e/h signal ratio as a function of the gate time clearly confirmed the predicted effect[3,6] . For LAr readout, the signal integration time is usually longer ($\sim 1\mu$s) and, therefore, $f_{\rm capt}$ may be up to $\sim$ 80% for sufficiently large detectors.

3.7 The e/h signal ratio

The e/h signal ratio was calculated in the way described in sect. 3.1. It was shown in sect. 3.2 - 3.6, that the results depend on a large number of factors, of which we recall:

a) The Z of the active and passive media (*e.g* for e/mip, γ/mip, $f_{\rm ion}$, $f_{\rm n}$).

b) The hydrogen content of the active medium (n/mip).

c) The saturation properties (kB value) of the active medium (ion/mip, n/mip).

d) The nuclear level structure of the absorber (n/mip).

e) The size of the detector ($f_{\rm capt} \rightarrow f_\gamma$).

f) The cross section for thermal neutron capture in the absorber (f_γ).

g) The signal integration time (f_γ).

h) The thickness of the passive layers (e/mip, γ/mip).

i) The thickness of the active layers (e/mip, γ/mip, ion/mip).

j) The sampling fraction (n/mip).

Because of the interesting consequences of the latter effect, e/h curves are presented as a function of the sampling fraction, or rather R_d, for a fixed choice of the readout thickness (figs. 13b, 14). These figures show that the e/h signal ratio for uranium calorimeters with hydrogenous readout decreases rather sharply with increasing R_d, *i.e.* with increasing absorber plate thickness. The e/h ratio can therefore be tuned through the sampling fraction, and for the hydrogenous materials shown (various plastic scintillators, TMP) an ideal sampling fraction ($e/h = 1$) exists.

The sensitivity of the e/h ratio to the sampling fraction depends on two factors:

i) The fraction of hydrogen atoms in the active medium. Since TMP contains more hydrogen atoms than plastic scintillator, the e/h signal ratio of TMP calorimeters is more sensitive to changes in the sampling fraction.

ii) Saturation of the active medium. Less saturation causes a larger sensitivity, and consequently leads to a larger optimal sampling fraction. This is illustrated in figure 14 , where the predictions for TMP readout are given for two different kB values. Contrary to plastic scintillator, the kB value has not been measured for soft protons in TMP, so far. The figure shows that this is a crucial parameter for the calorimeter performance.

For calorimeters with non-hydrogenous active layers (e.g. LAr, Si), the effect of the sampling fraction on the relative contribution of neutrons to the calorimeter signal (fig. 13a) is absent. The fact that e/h rises for small R_d values is caused by the effect of the absorber layer thickness on the electromagnetic response (fig. 5). It turned out that the e/h ratio depends quite sensitively on the contribution of captured neutrons to the hadronic calorimeter signal (sect. 3.6), which can be tuned through the signal integration time. Nevertheless, it looks as if the compensation condition cannot be reached for LAr.

For Si readout it might just be possible. The difference between LAr and Si comes from the fact that Si does not saturate in detecting the spallation protons (sect. 3.5) and, therefore, gives a larger response to the non-em shower component.

The calculations were performed for infinitely large detectors. We investigated how sensitive the predictions are with respect to the various assumptions that went into the calculations. In fact fig. 13b is an example of this. Other uncertainties concern $f_{\rm ion}$, $f_{\rm n}$ and the spallation proton spectrum (sect. 3.4, 3.5). It turned out that these uncertainties concerning details of the hadronic shower development may considerably affect the absolute value of the vertical scale, but *not* the variation of e/h with the sampling fraction, nor the difference between the various active materials. Therefore, the absolute e/h signal ratio for a given absorber/readout combination cannot be predicted from scratch more accurately than to within $5-10\%$, but one reliable experimental measurement will make possible a reliable prediction of the optimal configuration.

The experimental results obtained with uranium calorimeters so far seem to support this conclusion. In particular, the predicted trend of a decreasing e/h ratio for increasing R_d in the case of scintillator readout is experimentally very well confirmed. The same is true for the differences between scintillator and LAr. Experimental results for TMP and Si readout are unfortunately still lacking.

We also did extensive calculations for calorimeters with Pb or Fe absorber. The lead results are most interesting. The differences with uranium mainly concern the amount of energy carried by the soft-neutron component, because of the absence of fission and because of the fact that the Pb nucleus is less neutron-rich than uranium. Figure 13a shows that this can be compensated for by choosing a smaller sampling fraction (larger R_d). This increases n/mip and hence brings the contribution of neutrons to the calorimeter signal at the appropriate level. Again, this trick works only for hydrogenous readout materials. For scintillator, e/h was predicted to become 1.0 for $R_d \approx 4$, *i.e.* if the lead plates are made 4 times as thick as the scintillator plates.

In sect. 3.6 we saw that γ's from thermal neutron capture represent a considerable fraction of the total hadronic energy, since it is by emitting these γ's that the nuclei render

the binding energy lost when the neutrons were released. In plain lead calorimeters the contribution of this process to the signal will be negligible. The cross section for (n,γ) reactions is 0.17 b, against 2.7 b for uranium. This corresponds to a mean free path of $\sim$ 180 cm for a thermal neutron in lead (8 cm in U). Cadmium has a capture cross section of 2450 b. If one would add $\sim$ 1% Cd to the lead, thermal neutrons would be efficiently captured. This would in particular be interesting for LAr calorimeters with a long signal integration time. Also in U/LAr one might profit from adding a little Cd, since the energy released in neutron capture by Cd (9.0 MeV) is almost twice as large as in ^{238}U (4.8 MeV).

The calculations showed that even Fe calorimeters could be made compensating, at very small sampling fractions. Experimental data from the WA1 Collaboration seem to support this conclusion[4,7] .

A final word should be said about homogeneous hadron calorimeters. The mechanisms that are described in this section and that make compensating calorimeters possible, are based on the fact that we are dealing with *sampling* calorimeters: Only a (small) fraction of the shower energy is deposited in the active layers, and by carefully tuning variables one may equalize the em and non-em *response*. This does not work for homogeneous devices, like the fully sensitive liquid argon tank proposed by Ypsilantis[15] . In the non-em shower part inevitably losses will occur that cannot be compensated for, *e.g.* the binding energy required to release protons or nucleon aggregates from their nuclear environment. The $e/h^{\rm intr}$ signal ratio will, therefore, always have to be larger than 1.0 for such devices.

4. THE ENERGY RESOLUTION OF HADRON CALORIMETERS

After having discussed the e/h signal ratio and the factors that determine its value, we now return to the aim of this paper, *i.e.* trying to understand the energy resolution of hadron calorimeters, and the factors that limit their performance in this respect.

The energy resolution of a hadron calorimeter with separate passive and active layers is determined by four factors:

1) Sampling fluctuations.

2) Detector imperfections.

3) Deviations from $e/h^{\rm intr} = 1$.

4) The intrinsic energy resolution.

The sampling fluctuations were discussed in sect. 2. Fabjan *et. al.*[12] have measured their contribution to the energy resolution of Fe/LAr and U/LAr calorimeters. The results are usually quoted as[9]

$$\sigma_{\rm samp}/E = 0.09\sqrt{\frac{\Delta E({\rm MeV})}{E({\rm GeV})}}$$

where ΔE is the energy deposited by a mip in one sampling layer.

Detector imperfections will cause deviations from $1/\sqrt{E}$ scaling, and therefore limit the high-energy performance. It is believed that for well-designed calorimeters their contribution can be limited to $\sigma/E = 1\%$. Recently, HELIOS measured $\sigma/E = 1.9\%$ for the total energy distribution of reaction products from $^{16}{\rm O} + {\rm W}$ collisions at 3.2 TeV, at running conditions[3] . This impressive result supports the previous statement. In our calculations we assumed the detectors to be perfect.

As was shown in sect. 2, deviations from $e/h^{\rm intr} = 1$ contribute a constant term to the energy resolution σ/E. The value of this constant may be obtained from fig. 3a. In this section we will concentrate on the part that remains, *i.e.* on the intrinsic energy resolution for compensating calorimeters.

In hadron showers, a considerable fraction of the non-em energy is spent on nuclear binding energy losses, on average up to $\sim 40\%$ in high-Z materials. The fluctuations about this average are huge. This is illustrated in fig. 15a, where the binding energy lost in the various reactions that may occur when 1 GeV protons hit ^{238}U nuclei, is given. The total binding energy loss in a hadron shower (ΔB) is a convolution of many distributions

of this type. We estimated that the contribution of event-to-event fluctuations in ΔB to the energy resolution amounts to $(30-35\%)/\sqrt{E}$, if the effects of neutron- and γ-detection are neglected. However, these effects are very important.

The total kinetic energy carried by neutrons ($E_n^{\rm tot}$) is evidently correlated with ΔB (see fig. 15). A relatively large binding energy loss means that a relatively large fraction of the hadron energy is transferred to neutrons as well; detection of these particles corrects, at least partially, for the relatively small signal from ionizing particles in the event concerned, and vice versa. If the neutrons are detected with a good energy resolution themselves, *i.e.* if there is a strong correlation between $E_n^{\rm tot}$ and the neutron contribution to the calorimeter signal, the intrinsic resolution due to fluctuations in ΔB may be considerably reduced.

The energy resolution for neutron detection was studied with the same Monte Carlo package that was used to calculate the n/mip signal ratio (sect. 3.6). By transporting many neutrons through a given calorimeter structure, the signal distribution for a fixed $E_n^{\rm tot}$ was obtained. It turned out that the correlation between $E_n^{\rm tot}$ and the neutron contribution to the calorimeter signal may considerably improve, if elastic $n-p$ scattering in the active calorimeter layers occurs. The degree of correlation depends on the same factors that determined the n/mip signal ratio, *i.e.* on the hydrogen content, the kB value, and the sampling fraction. In addition, the thickness of the layers is important for the detection of the γ component.

With these results we calculated the total intrinsic energy resolution, assuming perfect correlation between ΔB and $E_n^{\rm tot}$. The validity of this assumption breaks down at low E and/or low $Z_{\rm abs}$. Results for uranium calorimeters are given in fig. 16. This figure shows that the intrinsic energy resolutions for practical detectors with hydrogenous readout material are considerably better than for LAr or Si, and may be as low as $20\%/\sqrt{E}$ for compensating calorimeters (note that the minima in the curves do not coincide with $e/h=1$). The same conclusion holds for calorimeters with other absorbers.

This yields a new and independent argument in favour of hydrogenous readout material: The energy resolution of a U/Si calorimeter, even if this combination can be made

compensating, will be inferior to plastic-scintillator or TMP calorimeters with $e/h = 1$.

The *total* hadronic energy resolution was computed as

$$\sigma/E = \sqrt{\frac{a_0^2 + a_1^2 \times t}{E}} + b$$

The intrinsic resolution (a_0) and the sampling fluctuations (a_1, proportional to the square root of the absorber layer thickness t), are added in quadrature. The constant term b vanishes for $e/h = 1$, and causes $\sigma/\sqrt{E}$ to be energy dependent in other cases. Figures 17-19 show some results of the calculations. Many more results are given in ref. 7. The figures show $\sigma/\sqrt{E}$ for 10 and 100 GeV, and the various contributions to it, for calorimeters with a given thickness of the active layers, as a function of the thickness of the absorber layers. The abcissa is plotted linear in the square root of the latter, which yields a straight line for the contribution of sampling fluctuations. Experimental results are included in the figures.

Figure 17 concerns uranium calorimeters with PMMA (polymethyl metacrylate, a plastic scintillator) readout. The total energy resolution reaches a minimum value for an absorber thickness close to the one for which $e/h = 1$. This is certainly true at high energies. At low energies, effects of sampling fluctuations and intrinsic contributions may slightly shift the optimal plate thickness. The curves for the total energy resolution at 10 and 100 GeV have a common point if $e/h = 1$: σ/E scales as $c/\sqrt{E}$, with $c = 0.32$ and 0.38 for 2.5 mm and 5 mm scintillator, respectively. These numbers are in good agreement with experimental values reported[2,3,16] . The results obtained by the WA78 Collaboration for non-optimal configurations[5] confirm the predicted violation of $c/\sqrt{E}$ scaling.

In fig. 18 results for U/LAr calorimeters are given. As for the e/h signal ratio, two cases were considered, $f_{\text{capt}} = 0.20$ and 0.80, respectively (see sect. 3.7). The predictions are rather sensitive to this parameter. If f_{capt} is increased, the energy resolution improves and $\sigma/\sqrt{E}$ becomes less energy dependent. Since $e/h \neq 1$ for all configurations, $\sigma/\sqrt{E}$ will always increase with E. The experimental results are in better agreement with the

low f_{capt} value. The small size of the test calorimeters with which they were obtained is likely to be (partly) responsible for this.

Figure 19 shows results for lead/plastic-scintillator calorimeters. As was discussed in sect. 3.7, this combination can be made compensating if the absorber layers are ~ 4 times as thick as the readout layers. Inspired by this prediction, Kötz *et. al.* from the ZEUS Collaboration tested a 10 mm Pb/2.5 mm plastic scintillator calorimeter[17]. They measured an energy resolution σ/E of $43\%/\sqrt{E}$ for pion detection, scaling with $1/\sqrt{E}$ over the whole energy range they scanned ($3 - 75\,\mathrm{GeV}$), while $41\%/\sqrt{E}$ was predicted. This is a remarkable result. Earlier, the same collaboration measured a considerably worse resolution ($60\%/\sqrt{E}$, fig. 19b) for a lead/plastic-scintillator calorimeter with a $4 - 5$ times larger sampling fraction[16] ($4 - 5\,\mathrm{mm}$ Pb/$5\,\mathrm{mm}$ scintillator). According to common wisdom, thicker absorber and thinner scintillator plates should have considerably deteriorated this result. Instead, an enormous improvement was observed, in agreement with our predictions.

5. OUTLOOK

The quality of experiments at a future supercollider will primarily be determined by the quality of the calorimetry. The calorimeters will have to deliver the information needed for reducing the event rates by ~ 7 orders of magnitude, while retaining those containing signatures of possible new physics. One will want to have the best possible calorimetry for that purpose. Energy resolution is an important issue in this respect, although by far not the only one. Three recent developments mark the considerable progress in this field:

i) The excellent energy resolutions measured by the HELIOS Collaboration at very high energies ($\sigma/E < 2\%$ at $3.2\,\mathrm{TeV}$).

ii) The experimental demonstration of a compensating lead calorimeter, with $\sigma/E = 43\%/\sqrt{E}$.

iii) The fact that ii) confirmed a theoretical prediction.

The first result implies that one may successfully aim for hadron calorimetry at the 1% precision level, for experiments at a multi-TeV machine. The second result shows that this goal can be achieved without uranium. The third result means that we understand *how* to achieve this goal.

In order to reach this level of precision, the calorimeter should have $e/h^{\rm intr} = 1$ to within $\sim$ 5%. This is definitely possible for four combinations: U/plastic-scintillator, Pb/plastic-scintillator, U/warm-liquid and Pb/warm-liquid. In all these cases energy resolutions $\sigma/E \approx 30\%/\sqrt{E}$ seem possible for practical detectors. Compensation can probably also be reached for U/LAr if a substantial fraction (more than 10%) of methane can be added, and for U/Si if the silicon is sandwiched between thin foils of hydrogenous material, *e.g.* polyethylene[18] . The energy resolution is expected to be considerably worse for these combinations, $\sim 50\%/\sqrt{E}$. In the first case this is due to the small sampling fraction (thick U-plates) needed, in the second case the absence of the effects that compensate for fluctuations in the nuclear binding energy loss limit the energy resolution[19] .

An essential condition for achieving good energy resolutions is also that the calorimeter structure be the same throughout the complete sensitive volume. The energy resolution of the U/TMP calorimeter being built by the UA1 Collaboration[20] will, expectedly, not nearly be as good as the HELIOS and ZEUS ones, if only because of the fact that it is longitudinally subdivided into sections with very different sampling fractions (*i.e.* $e/h^{\rm intr}$ values).

Another important criterion for choosing a particular calorimeter will be compactness. In this respect it is interesting to remark, that the effective nuclear interaction length (λ_{int}^{eff}) of *compensating* uranium and lead calorimeters using the same readout are practically the same, because of the quite different sampling fractions needed for compensation. In spite of its much larger density, uranium does not give any advantage in this respect. If only because of the well-known disadvantages of uranium, the lead alternatives deserve to be thoroughly explored[21] . For plastic scintillator, λ_{int}^{eff} amounts

to $\sim$ 20 cm. For TMP, λ_{int}^{eff} depends sensitively on the kB saturation constant, but is likely to be considerably larger than 20 cm. Silicon readout yields the most compact devices ($\lambda_{int}^{eff} \approx 15$ cm for U/Si).

Other important selection criteria concern the hermiticity, granularity, charge collection time, radiation resistance and calibration of the candidate calorimeter. The latter may well turn out to be the major limiting factor in the era of high resolution calorimetry.

Hadron calorimetry has become a mature scientific activity. The R&D activities needed for designing future detectors will get a solid basis.

REFERENCES

1) C.W. Fabjan and W.J. Willis, in Proceedings of the Calorimeter Workshop, Batavia Illinois (1975), p. 1, M. Atac, ed.

2) T. Akesson *et al.* Nucl. Instr. and Meth. **A241** (1985) 17.

3) T. Akesson *et al.*, Performance of the Uranium/Plastic Scintilator Calorimeter at CERN, to be published.

4) See for example H. Abramowicz *et al.*, Nucl. Instr. and Meth. **180** (1981) 429.

5) M. de Vincenzi *et al.*, Nucl. Instr. and Meth. **A243** (1986) 348.

6) H. Brũckmann and H. Kowalski, The Dependence of Calorimeter Responses on the Gate Width, DESY, Hamburg, ZEUS - Internal Note 86 / 026 (1986).

7) R. Wigmans, On the Energy Resolution of Uranium and Other Hadron Calorimeters, CERN-EP/86-141 (1986), accepted for publication in Nucl. Instr. and Meth.

8) U. Amaldi, Physica Scripta **23** (1981)409.

9) C.W. Fabjan and T. Ludlam, Ann. Rev. Nucl. Part. Sci. **32** (1982) 335.

10) C. Leroy, Y. Sirois and R. Wigmans, Nucl. Instr. and Meth. **A252** (1986) 4.

11) V.M. Gorbachev, Y.S. Zamyathin and A.A. Lbov, Nuclear Reactions in Heavy Elements, a Data Handbook (Pergamon Press, London, 1980).

12) C.W. Fabjan *et. al.*, Nucl. Instr. and Meth. **141** (1977) 61.

13) Y. Galaktionov *et. al.*, Nucl. Instr. and Meth. **A251** (1986) 258.

14) H. Brũckmann, Hadron Sampling Calorimetry, preprint DESY/86-155 (1986).

15) T. Ypsilantis, Contribution to this Conference.

16) J. Engelen and H. Tiecke, Performance of a Hadron Test Calorimeter for the ZEUS Experiment, preprint NIKHEF-H/86-18 (1986).

17) R. Klanner, Test Results for the ZEUS Calorimeter, Contribution to this Conference.

18) T. Akesson *et al.*, Detection of Jets with Calorimeters at Future Accelerators, Proc. of the Workshop on Physics at Future Accelerators, La Thuile and CERN (1987); CERN-EP/87-88.

19) R. Wigmans, Signal Equalization and Energy Resolution for Uranium/Silicon Hadron Calorimeters, to be published.

20) see M. Albrow *et al.*, Performance of a Uranium/Tetramethylpentane Electromagnetic Calorimeter, CERN-EP/87-55 (1987).

21) P. Jenni *et al.*, The High Resolution Spaghetti Hadron Calorimeter, NIKHEF-H/87-07 (1987).

FIGURE CAPTIONS

1. The calorimeter response to the em and non-em components of a hadron shower.

2. Experimental data obtained with an iron/plastic-scintillator calorimeter (the open circles), and with uranium/plastic-scintillator (full circles). The crosses represent the off-line weighted iron results. Data are given on energy resolution (a) and linearity (b) as a function of energy.

3. Monte Carlo simulation of the effects of $e/h \neq 1$ on the energy resolution and signal linearity of hadron calorimeters.

4. The fraction of the energy of a 10 GeV electron shower, that is deposited through ionization by electrons and positrons slower than 1 or 4 MeV, or faster than 20 MeV, as a function of the Z-value of the calorimeter absorber. Results from EGS4 Monte-Carlo simulations.

5. The e/mip signal ratio as a function of the thickness of the active (a) and passive (b) layers, for uranium calorimeters. Results from EGS4 calculations.

6. The effect of stainless steel wrapping of the absorber plates on the e/mip value of a uranium/plastic-scintillator calorimeter. The vertical scale is normalized to the case where no steel is applied. Results from EGS4 calculations.

7. The γ/mip signal ratio as a function of E_γ, for a uranium/plastic-scintillator calorimeter. Results from EGS4 calculations.

8. The energy deposit and the calorimeter signal for stopping protons relative to mip's, as a function of the proton energy, for a 3 mm U/ 2.5 mm plasic scintillator calorimeter.

9. The cross sections for neutron-induced reactions on ^{238}U (a) and hydrogen (b) nuclei.

10. The longitudinal distributions of ^{239}Np nuclei (from neutron capture in ^{238}U), produced by hadron showers in various calorimeter configurations.

11. The various forms in which the kinetic neutron energy is deposited in a 3 mm U/3 mm plastic-scintillator calorimeter. Because of fission contributions, the total energy can be larger than 100%.

12. The response of a uranium gas-sampling calorimeter to pions and electrons, for different gases. Data from ref. 13.

13. The signal ratio n/mip split up in its components, for U/plastic-scintillator calorimeters, as a function of the ratio of the thicknesses of passive and active layers R_d (a). The signal ratio e/h as a function of R_d, assuming that 0% , 20% or 100% of the γ's released in thermal neutron capture contribute to the calorimeter signal (b).

14. The signal ratio e/h for uranium calorimeters employing different readout materials, as a function of the ratio of the thicknesses of absorber and readout layers. Results of experimental measurements are included.

15. The binding energy lost in spallation reactions induced by 1 GeV hadrons on ^{238}U nuclei (a), and the number of neutrons produced in such reactions (b). Results of calculations described in ref. 7.

16. The contribution of fluctuations in nuclear binding energy loss to the intrinsic resolution of various types of uranium calorimeters, as a function of the ratio of the thicknesses of the passive and active layers.

17. The total energy resolution and the various factors contributing to it, for detection of 10 and 100 GeV hadrons in U/PMMA calorimeters, as a function of the uranium plate thickness. The thickness of the scintillator plates amounts to 2.5 mm (a) or 5 mm (b). The numbers in brackets denote other energies at which experimental results were reported.

18. The total energy resolution and the various factors contributing to it, for detection of 10 and 100 GeV hadrons in U/Lar calorimeters, as a function of the uranium plate thickness. The liquid argon gap is 2.5 mm wide. The calculations assume that 20% (a) or 80% (b) of the thermalized neutrons are captured in the detector and contribute to the calorimeter signal.

19. The total energy resolution and the various factors contributing to it, for detection of 10 and 100 GeV hadrons in Pb/PMMA calorimeters, as a function of the thickness of the lead plates. The thickness of the scintillator plates is 2.5 mm (a) or 5 mm (b).

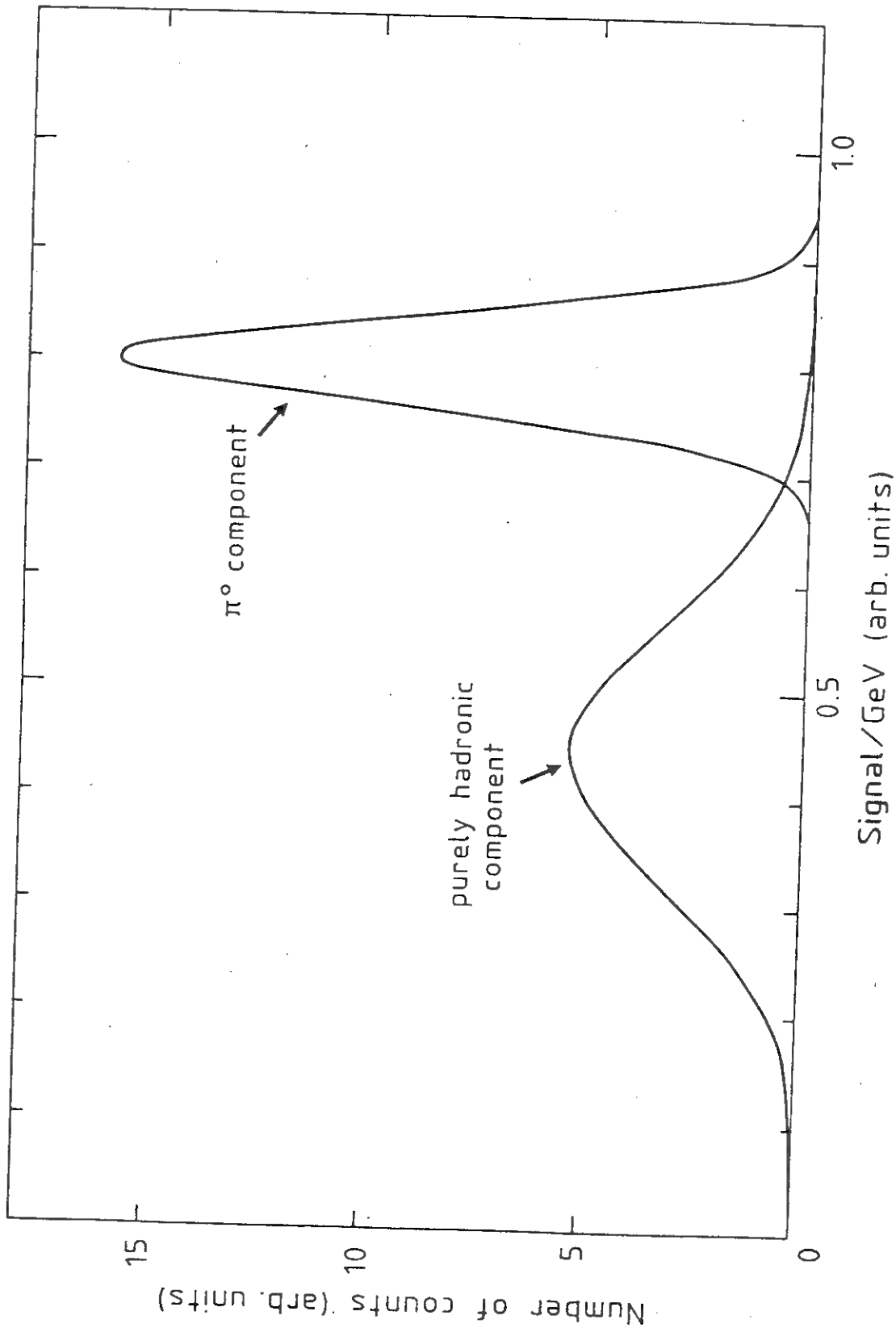
π° component
purely hadronic component
Number of counts (arb. units)
Signal/GeV (arb. units)
0
5
10
15
0.5
1.0

Figure 1

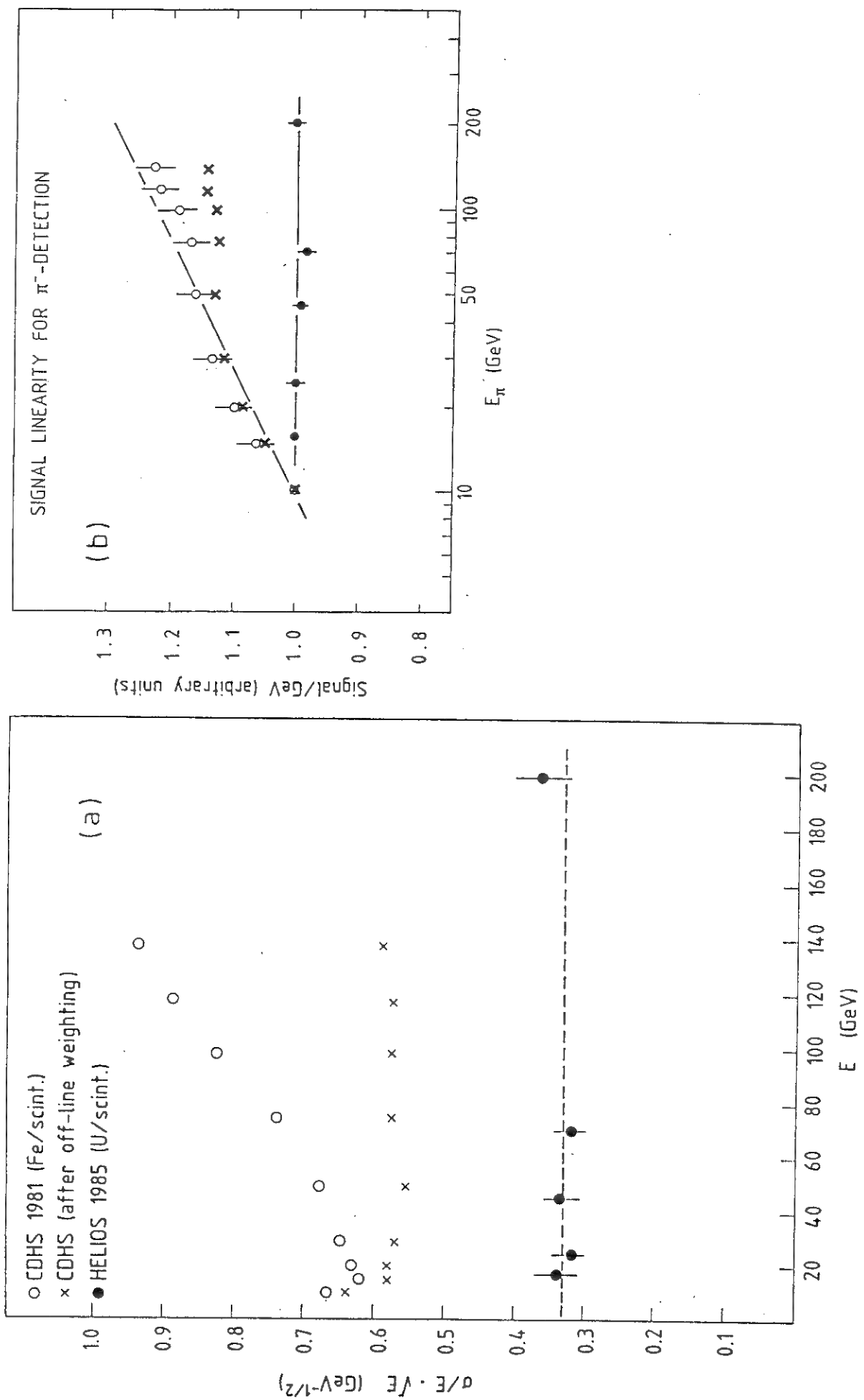
SIGNAL LINEARITY FOR π⁻-DETECTION
(b)
Signal/GeV (arbitrary units)
1.3
1.2
1.1
1.0
0.9
0.8
10
50
100
200
E_π (GeV)
(a)
○ CDHS 1981 (Fe/scint.)
× CDHS (after off-line weighting)
● HELIOS 1985 (U/scint.)
$\sigma/E \cdot \sqrt{E}$ (GeV$^{-1/2}$)
1.0
0.9
0.8
0.7
0.6
0.5
0.4
0.3
0.2
0.1
20
40
60
80
100
120
140
160
180
200
E (GeV)

Figure 2

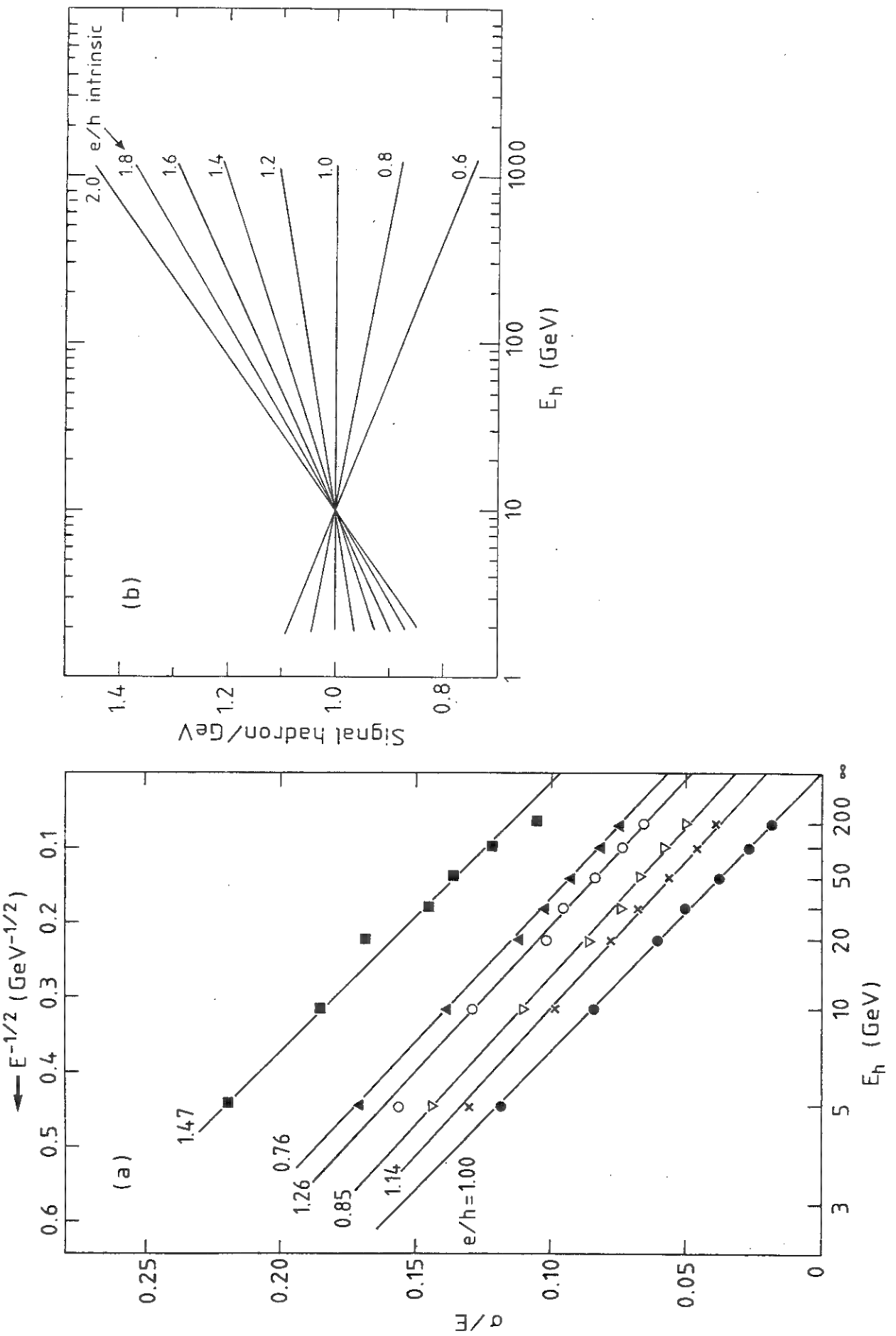
(a)
1.47
0.76
1.26
0.85
1.14
e/h=1.00
σ/E
E^-1/2 (GeV^-1/2)
E_h (GeV)
(b)
e/h intrinsic
2.0
1.8
1.6
1.4
1.2
1.0
0.8
0.6
Signal hadron/GeV
E_h (GeV)

Figure 3

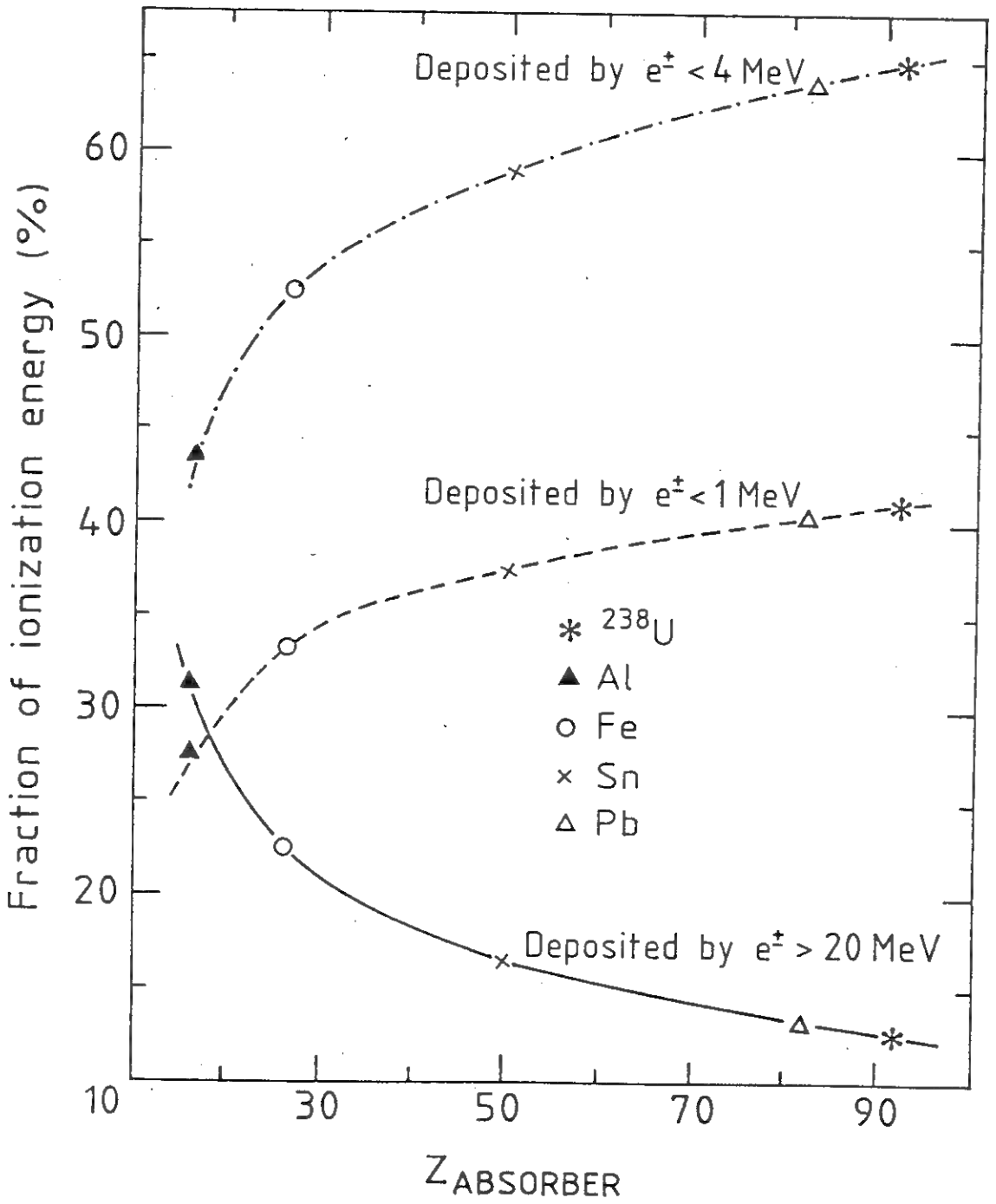
Deposited by $e^{\pm} < 4$ MeV
Deposited by $e^{\pm} < 1$ MeV
Deposited by $e^{\pm} > 20$ MeV
* ^{238}U
▲ Al
o Fe
× Sn
Δ Pb
Fraction of ionization energy (%)
60
50
40
30
20
10
30
50
70
90
$Z_{ABSORBER}$

Figure 4

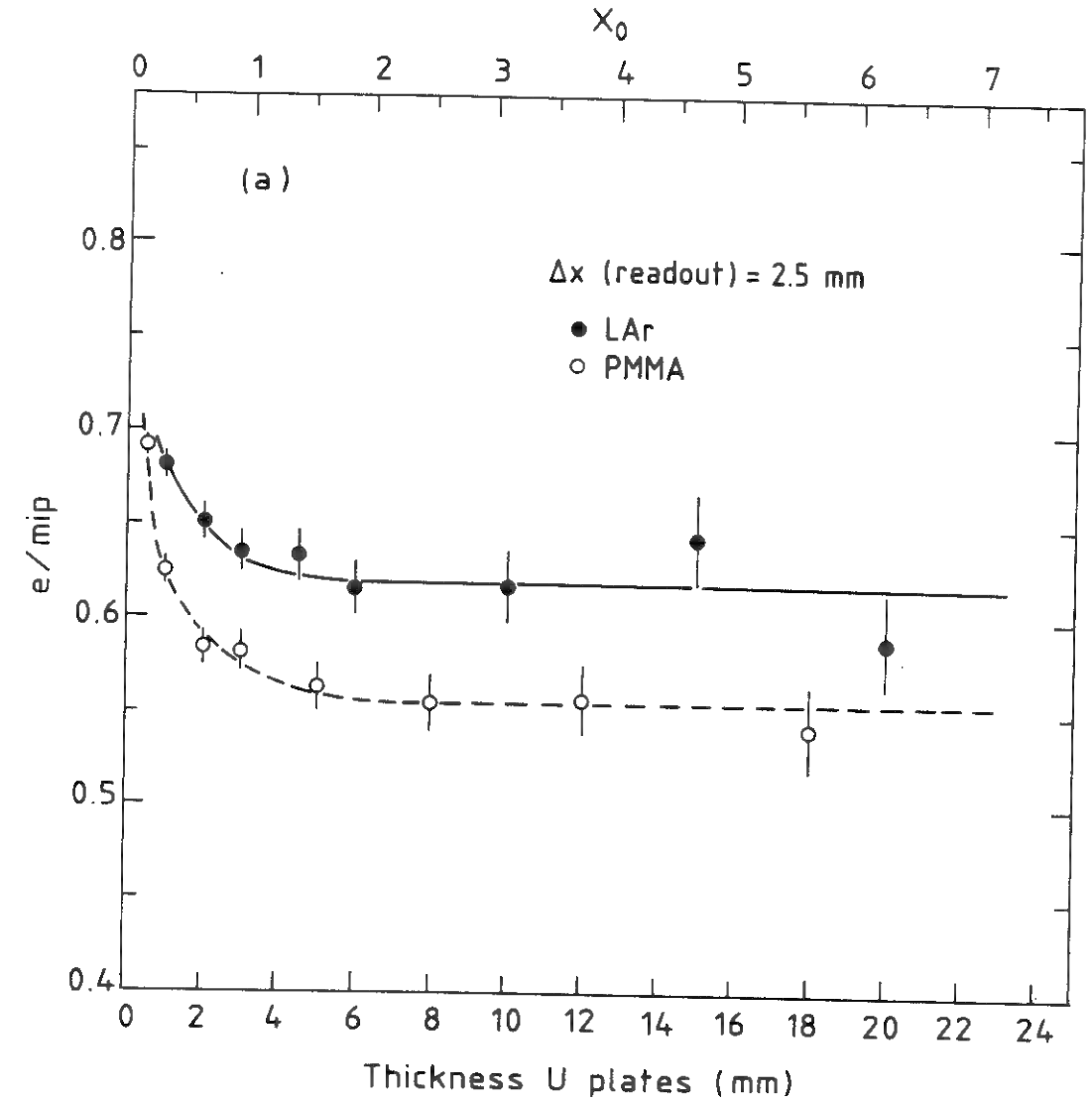
X0
0 1 2 3 4 5 6 7
(a)
Δx (readout) = 2.5 mm
LAr
PMMA
e / mip
0.8
0.7
0.6
0.5
0.4
0 2 4 6 8 10 12 14 16 18 20 22 24
Thickness U plates (mm)

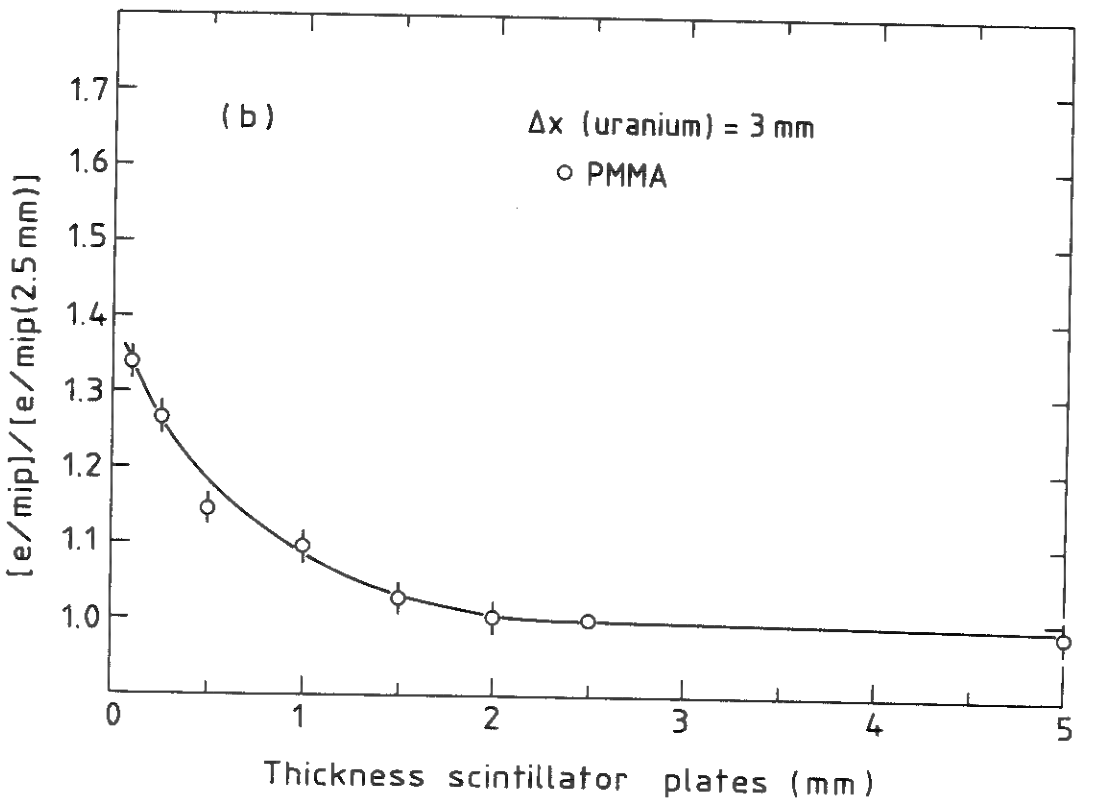
(b)
Δx (uranium) = 3 mm
PMMA
[e/mip]/[e/mip(2.5 mm)]
1.7
1.6
1.5
1.4
1.3
1.2
1.1
1.0
0 1 2 3 4 5
Thickness scintillator plates (mm)

Figure 5

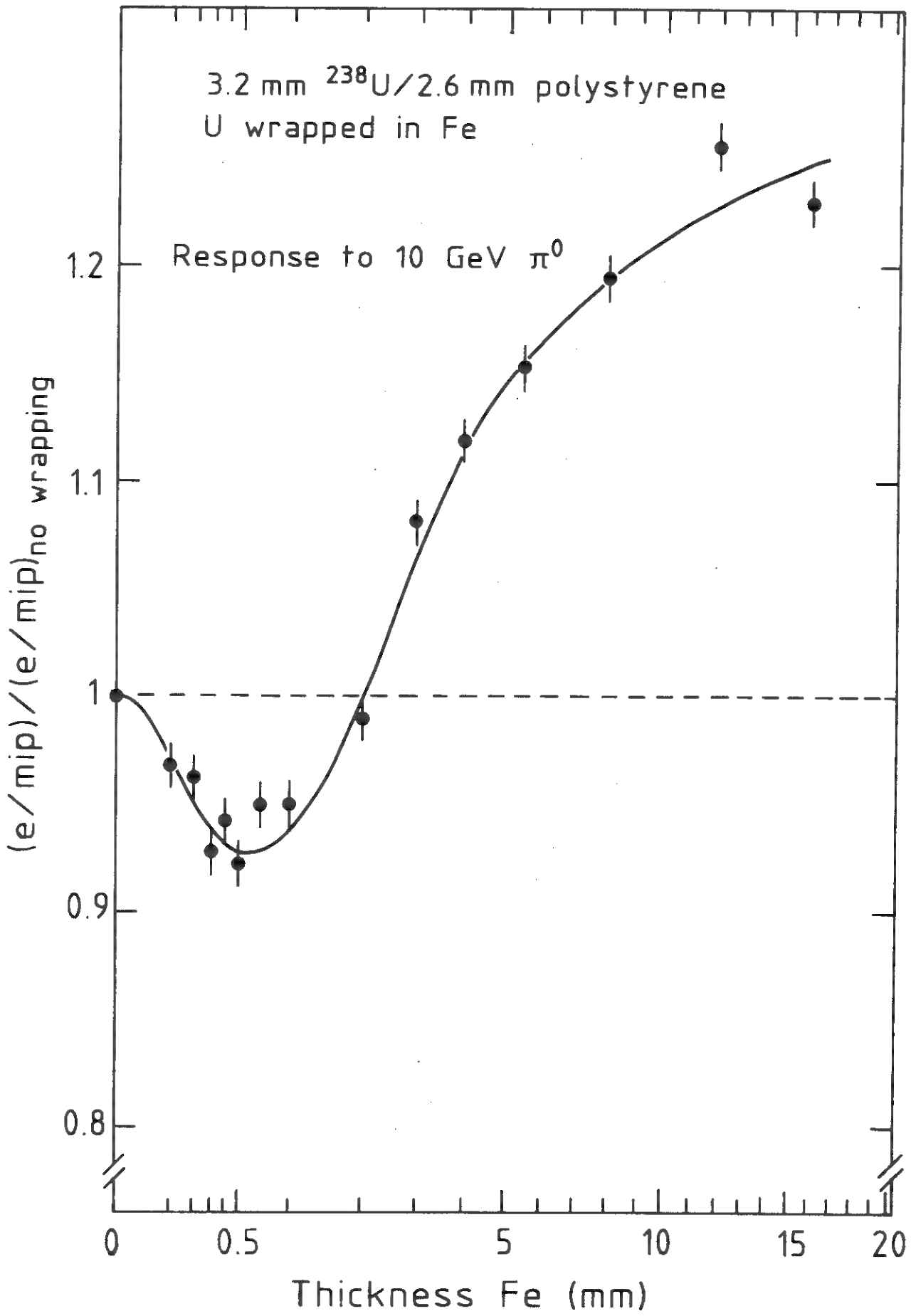
3.2 mm ^{238}U/2.6 mm polystyrene
U wrapped in Fe
Response to 10 GeV π^0
$(e/mip)/(e/mip)_{no\ wrapping}$
1.2
1.1
1
0.9
0.8
0
0.5
5
10
15
20
Thickness Fe (mm)

Figure 6

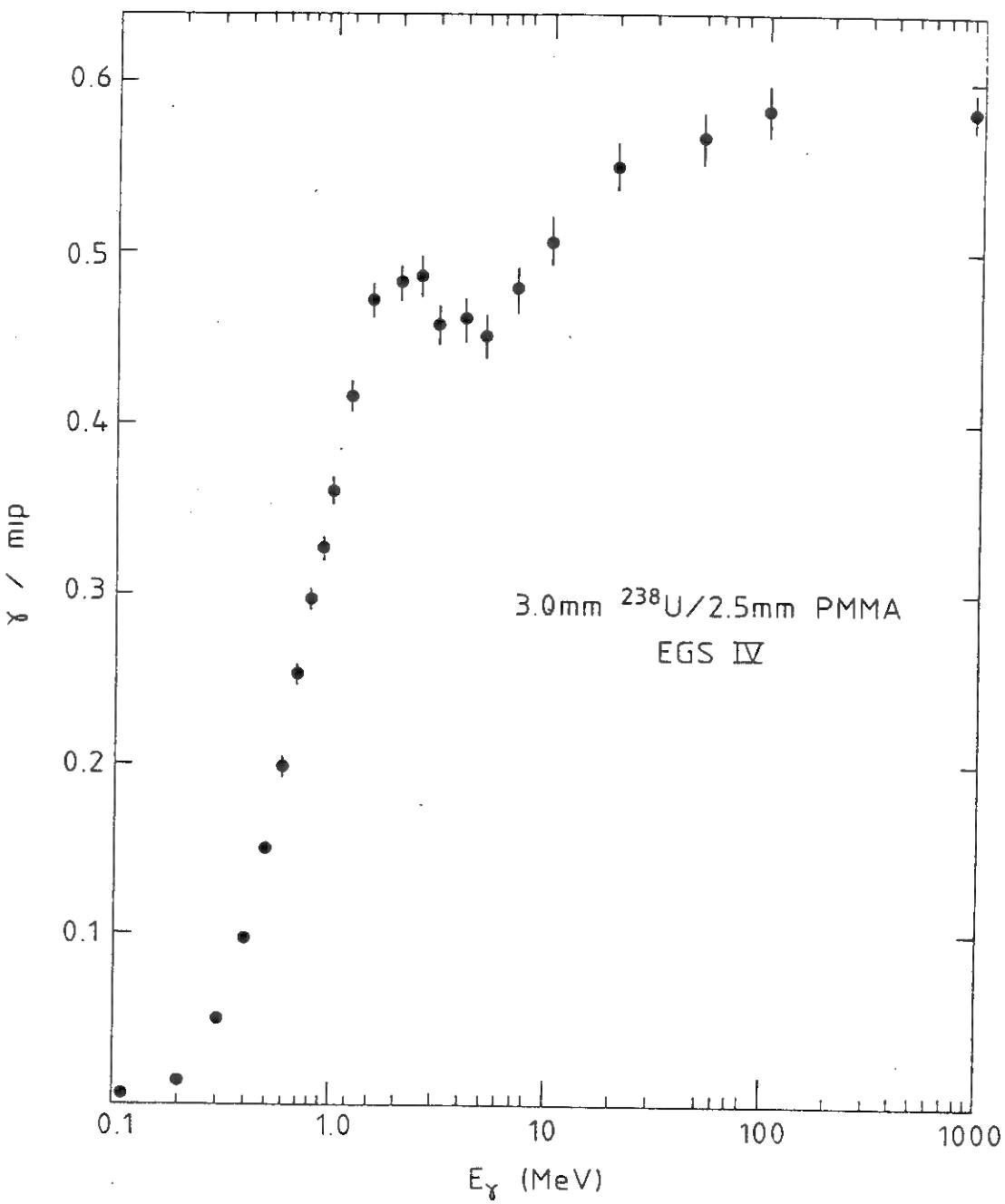
0.6
0.5
0.4
0.3
0.2
0.1
γ / mip
3.0mm ^{238}U/2.5mm PMMA
EGS IV
0.1
1.0
10
100
1000
E_γ (MeV)

Figure 7

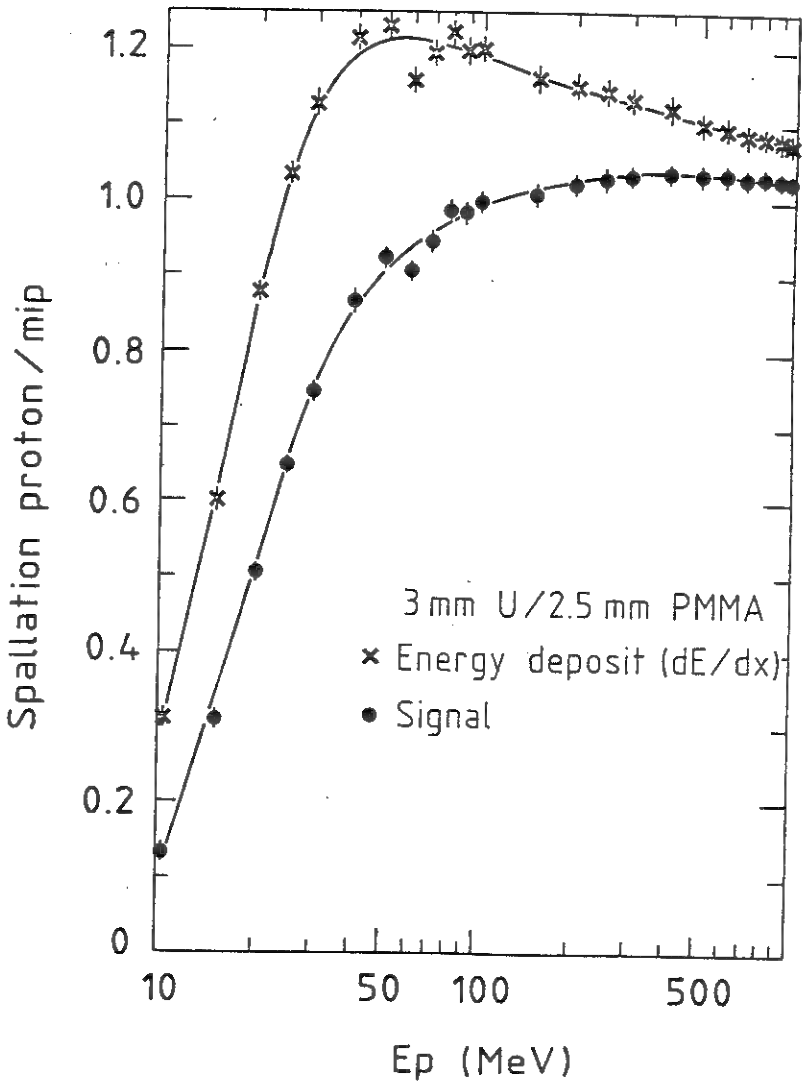
Spallation proton / mip
1.2
1.0
0.8
0.6
0.4
0.2
0
10
50
100
500
Ep (MeV)
3 mm U / 2.5 mm PMMA
× Energy deposit (dE/dx)
• Signal

Figure 8

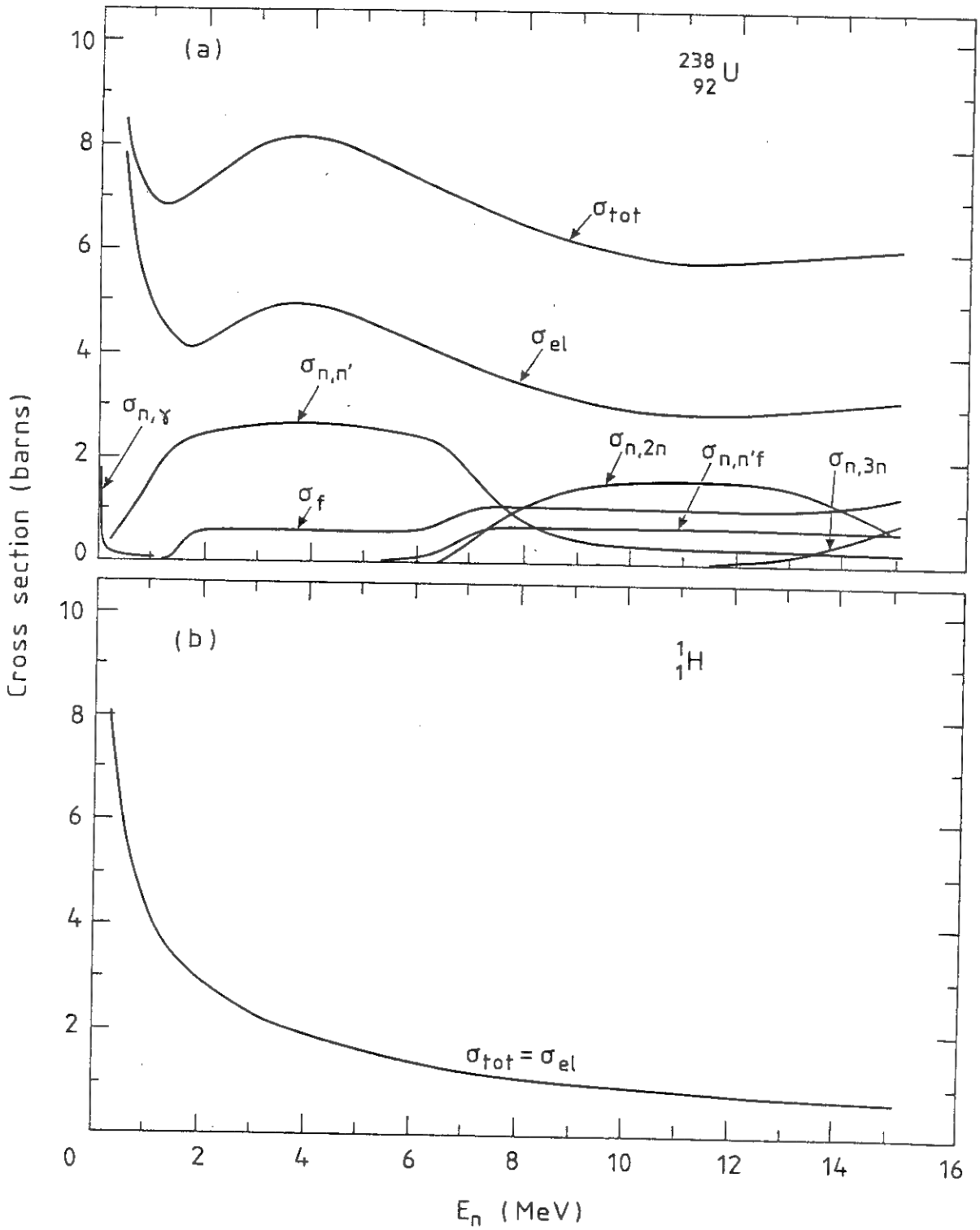
(a)
$^{238}_{92}U$
σ_{tot}
σ_{el}
$\sigma_{n,n'}$
$\sigma_{n,\gamma}$
$\sigma_{n,2n}$
$\sigma_{n,n'f}$
$\sigma_{n,3n}$
σ_f
(b)
$^{1}_{1}H$
$\sigma_{tot} = \sigma_{el}$
Cross section (barns)
E_n (MeV)

Figure 9

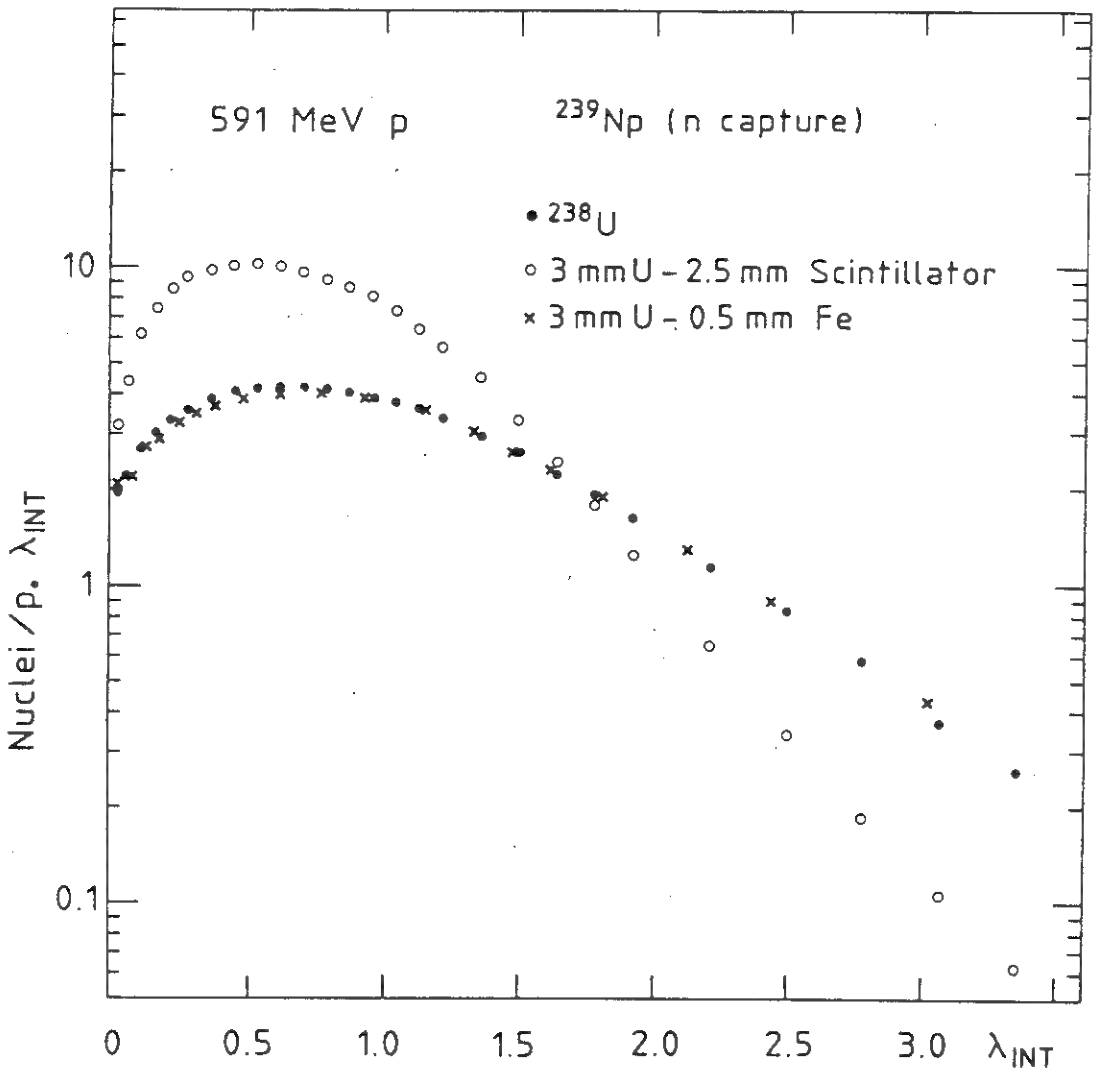
591 MeV p
239Np (n capture)
• 238U
○ 3 mm U - 2.5 mm Scintillator
× 3 mm U - 0.5 mm Fe
Nuclei / p. λINT
10
1
0.1
0
0.5
1.0
1.5
2.0
2.5
3.0
λINT

Figure 10

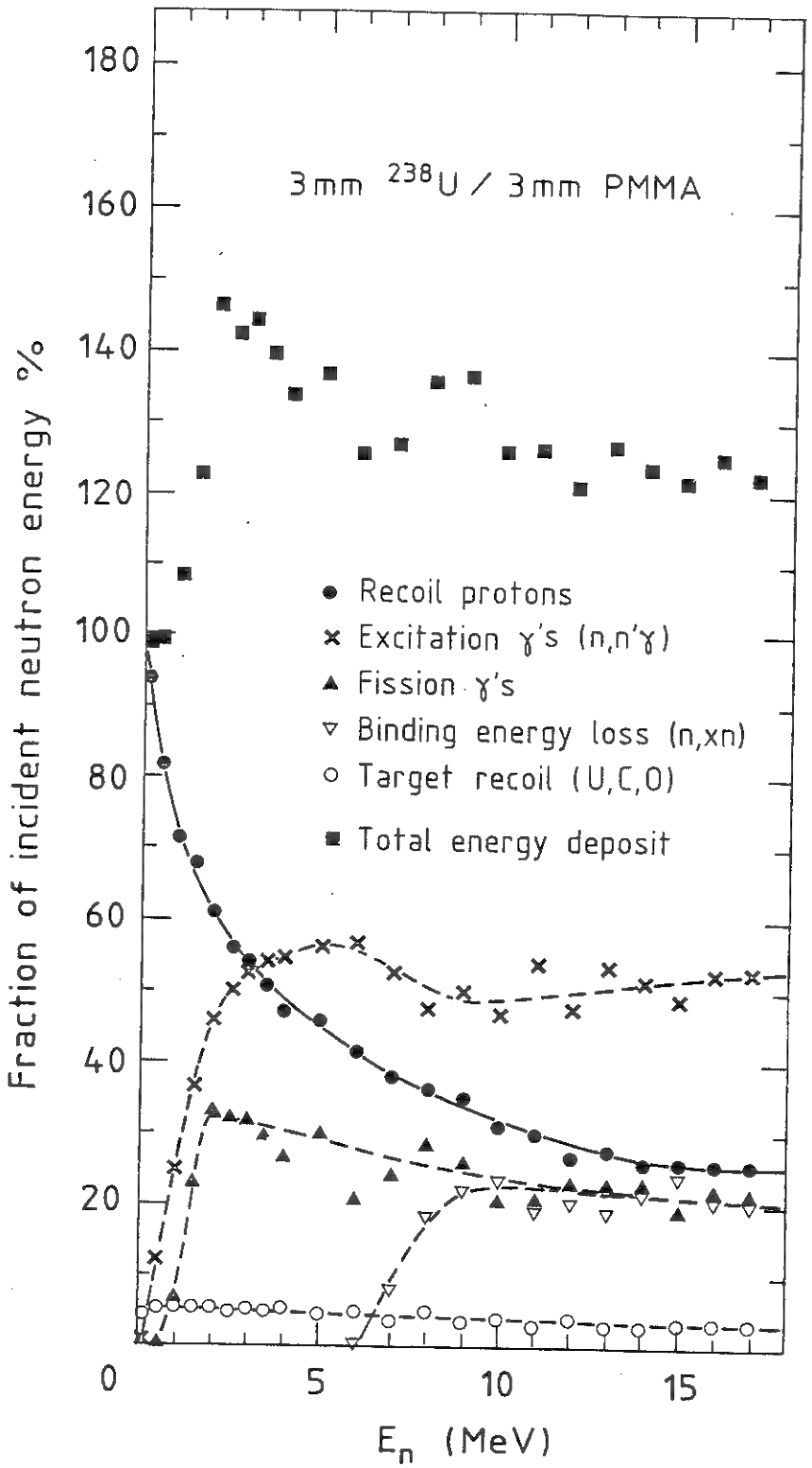
3mm ^{238}U / 3mm PMMA
Recoil protons
Excitation γ's (n,n'γ)
Fission γ's
Binding energy loss (n,xn)
Target recoil (U,C,O)
Total energy deposit
Fraction of incident neutron energy %
E_n (MeV)
0
20
40
60
80
100
120
140
160
180
5
10
15

Figure 11

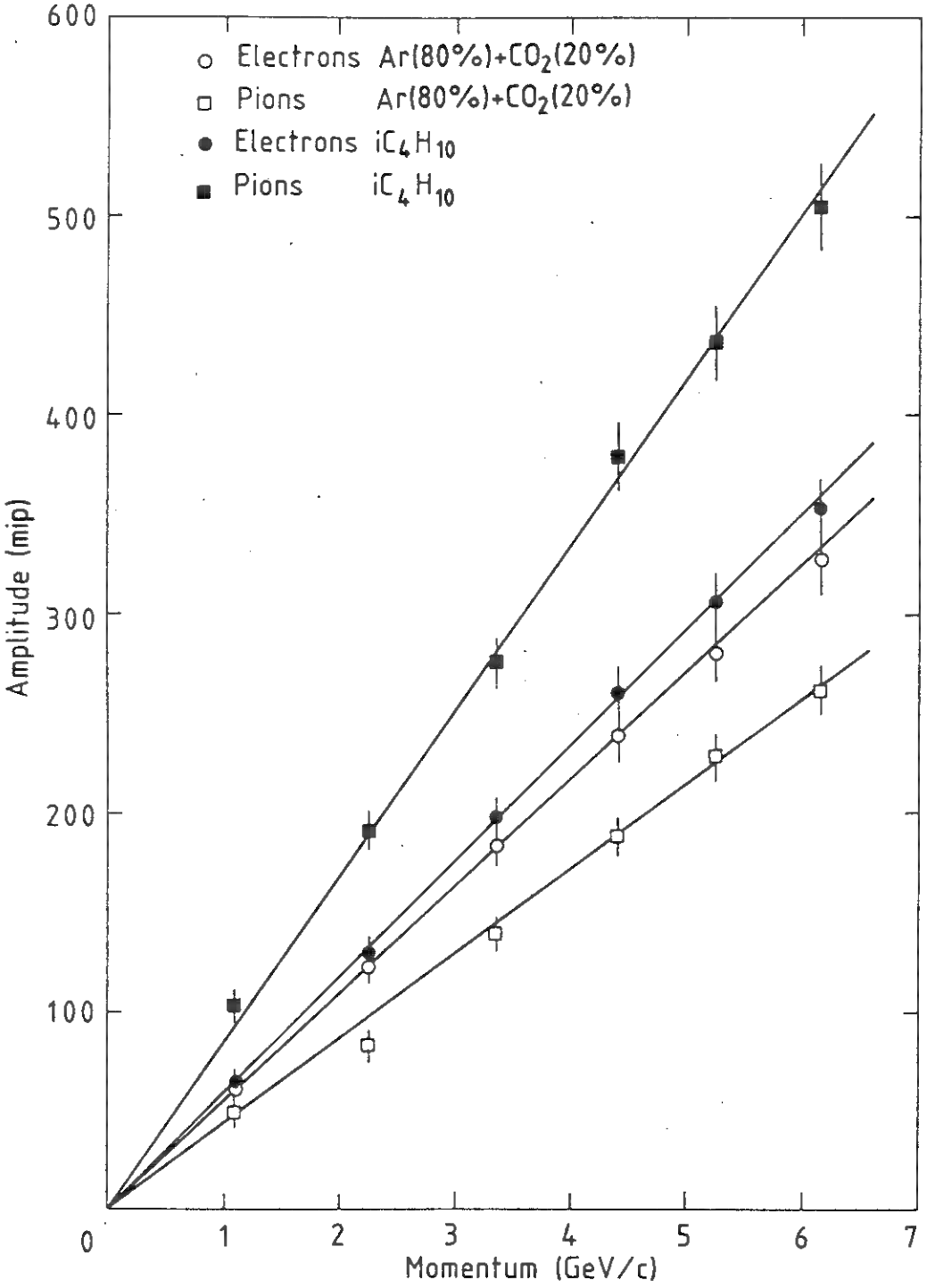
Electrons Ar(80%)+CO2(20%)
Pions Ar(80%)+CO2(20%)
Electrons iC4H10
Pions iC4H10
Amplitude (mip)
Momentum (GeV/c)
0
100
200
300
400
500
600
1
2
3
4
5
6
7

Figure **12**

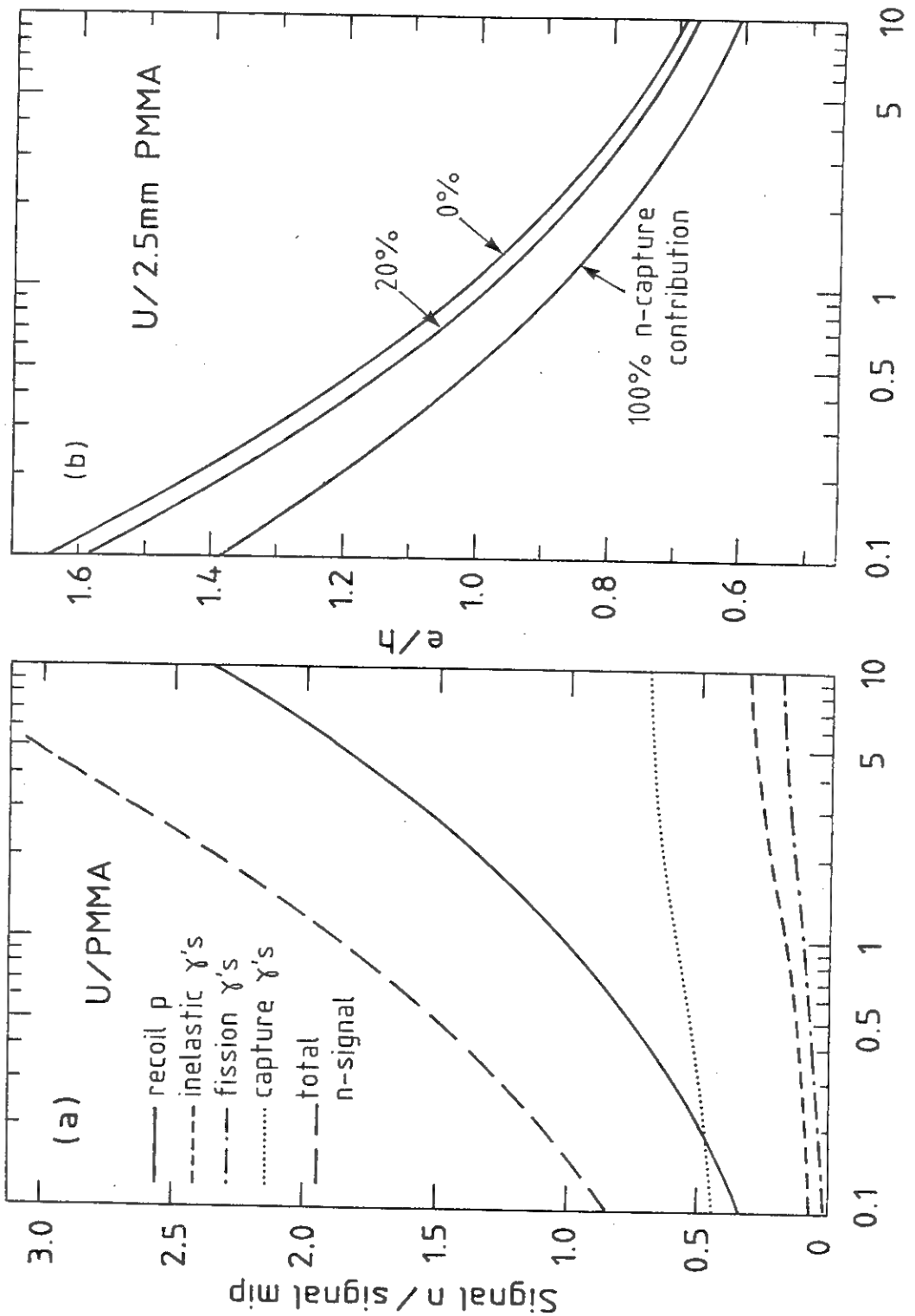
(a)
U/PMMA
recoil p
inelastic γ's
fission γ's
capture γ's
total
n-signal
Signal n / signal mip
R_d
(b)
U/2.5mm PMMA
20%
0%
100% n-capture contribution
e/h
R_d

Figure 13

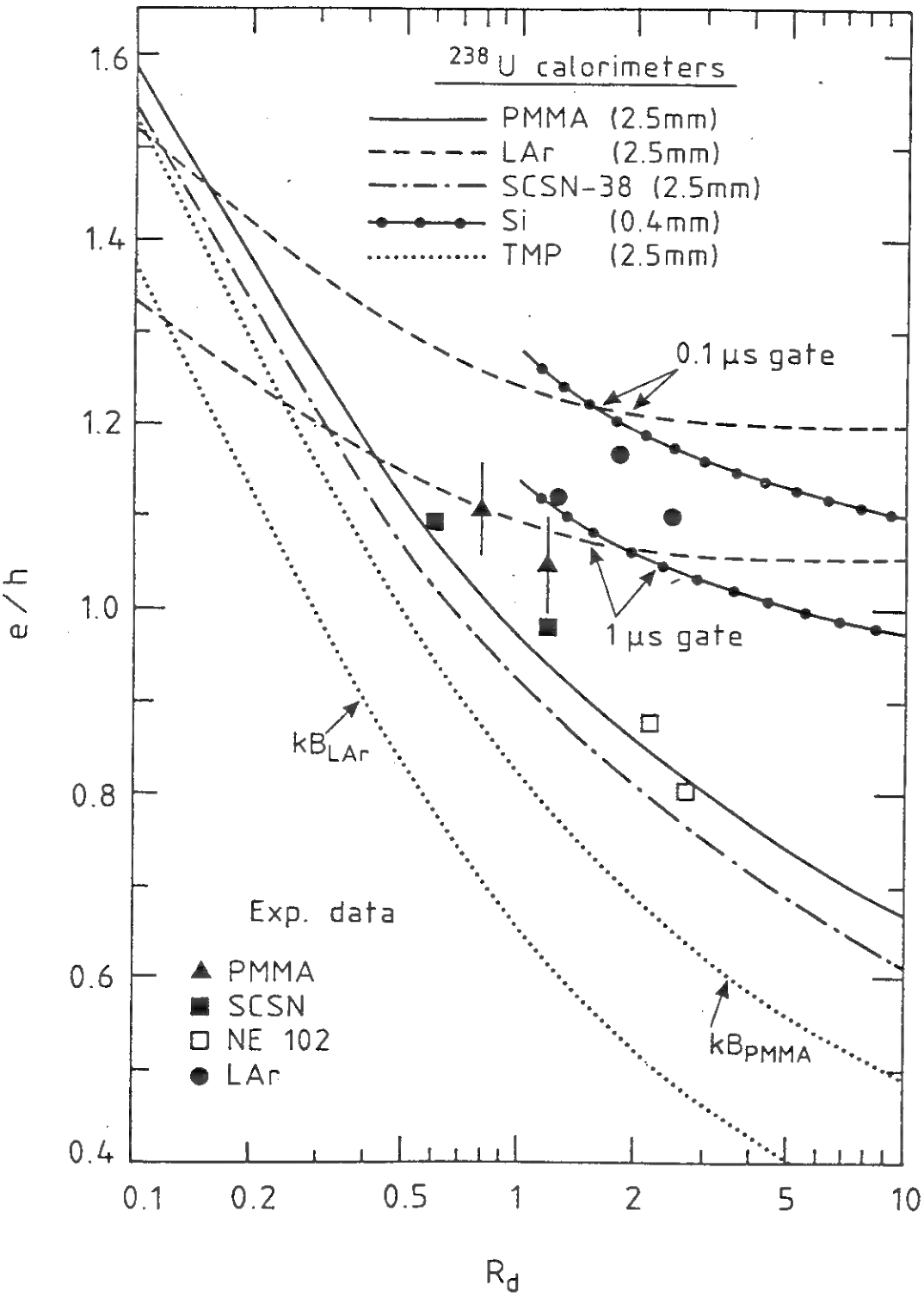
^{238}U calorimeters
PMMA (2.5mm)
LAr (2.5mm)
SCSN-38 (2.5mm)
Si (0.4mm)
TMP (2.5mm)
0.1 µs gate
1 µs gate
kB$_{LAr}$
kB$_{PMMA}$
Exp. data
PMMA
SCSN
NE 102
LAr
e / h
R$_d$
1.6
1.4
1.2
1.0
0.8
0.6
0.4
0.1
0.2
0.5
1
2
5
10

Figure 14

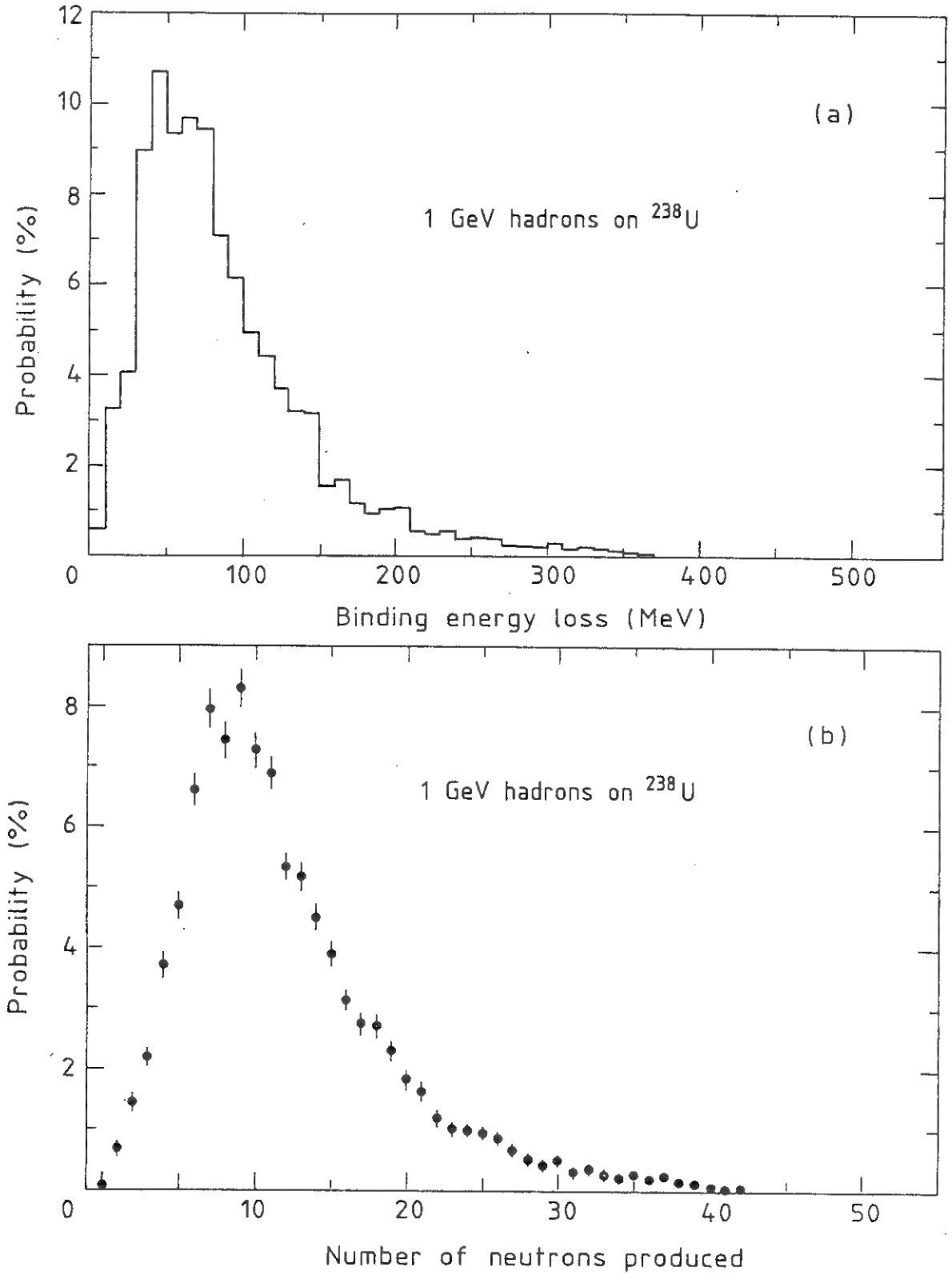
(a)
1 GeV hadrons on ^{238}U
Probability (%)
Binding energy loss (MeV)
(b)
1 GeV hadrons on ^{238}U
Probability (%)
Number of neutrons produced

Figure 15

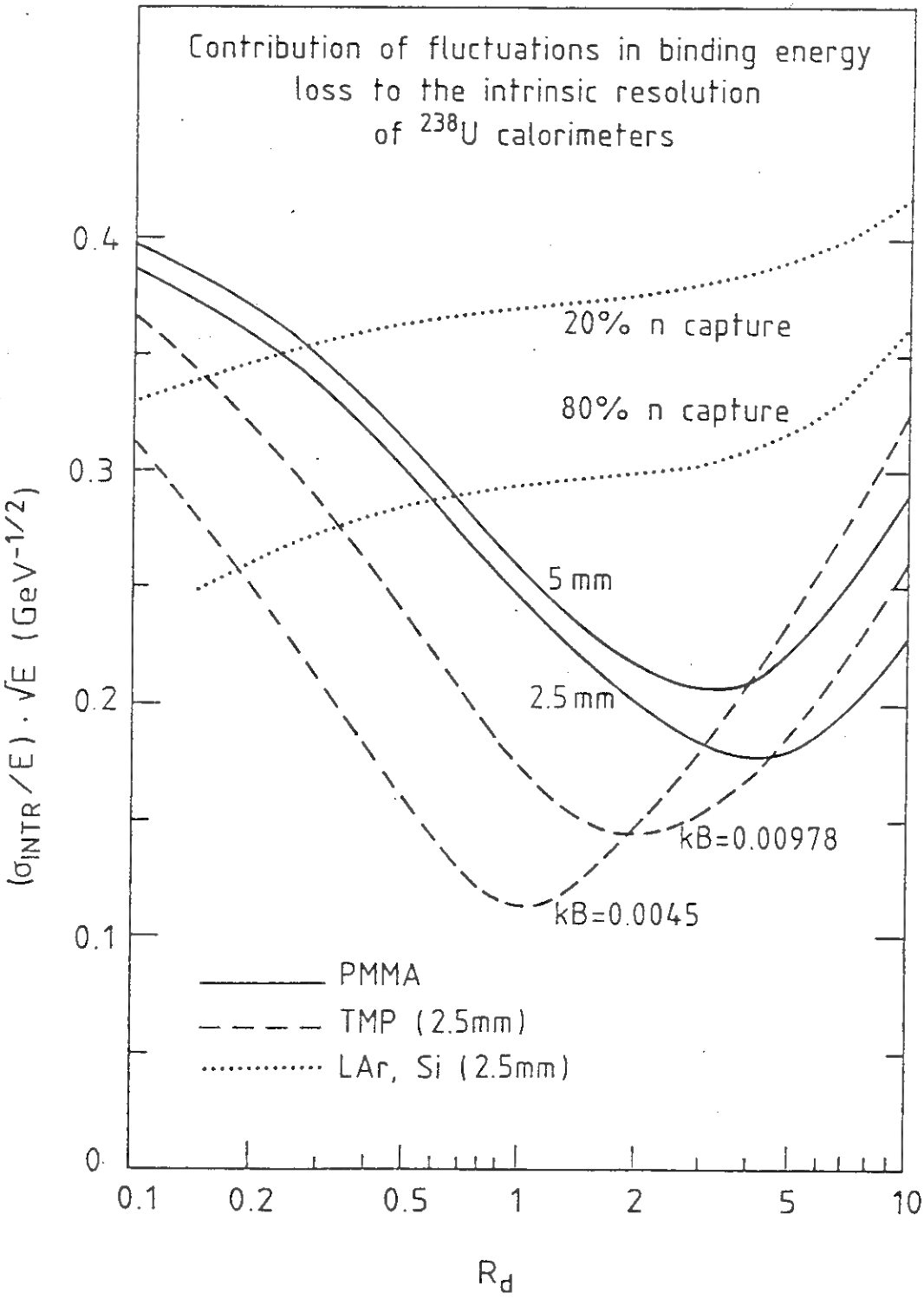
Contribution of fluctuations in binding energy
loss to the intrinsic resolution
of ^{238}U calorimeters
$(\sigma_{INTR}/E)\cdot\sqrt{E}$ (GeV$^{-1/2}$)
0.4
0.3
0.2
0.1
0
20% n capture
80% n capture
5 mm
2.5 mm
kB=0.00978
kB=0.0045
PMMA
TMP (2.5mm)
LAr, Si (2.5mm)
0.1
0.2
0.5
1
2
5
10
R_d

Figure 16

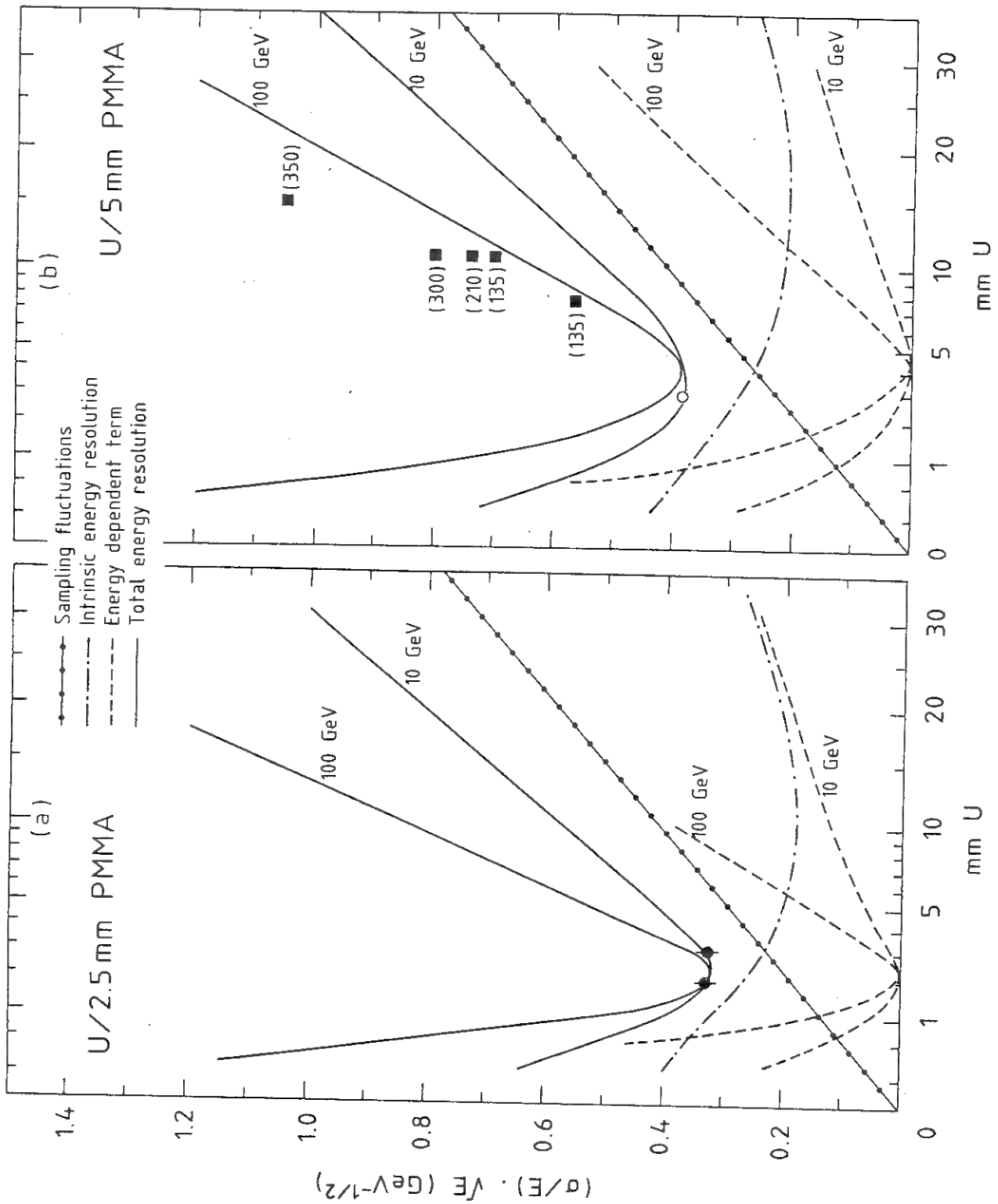
(a)
U/2.5mm PMMA
(b)
U/5mm PMMA
Sampling fluctuations
Intrinsic energy resolution
Energy dependent term
Total energy resolution
100 GeV
10 GeV
(350)
(300)
(210)
(135)
(135)
(σ/E) · √E (GeV-1/2)
mm U
mm U

Figure 17

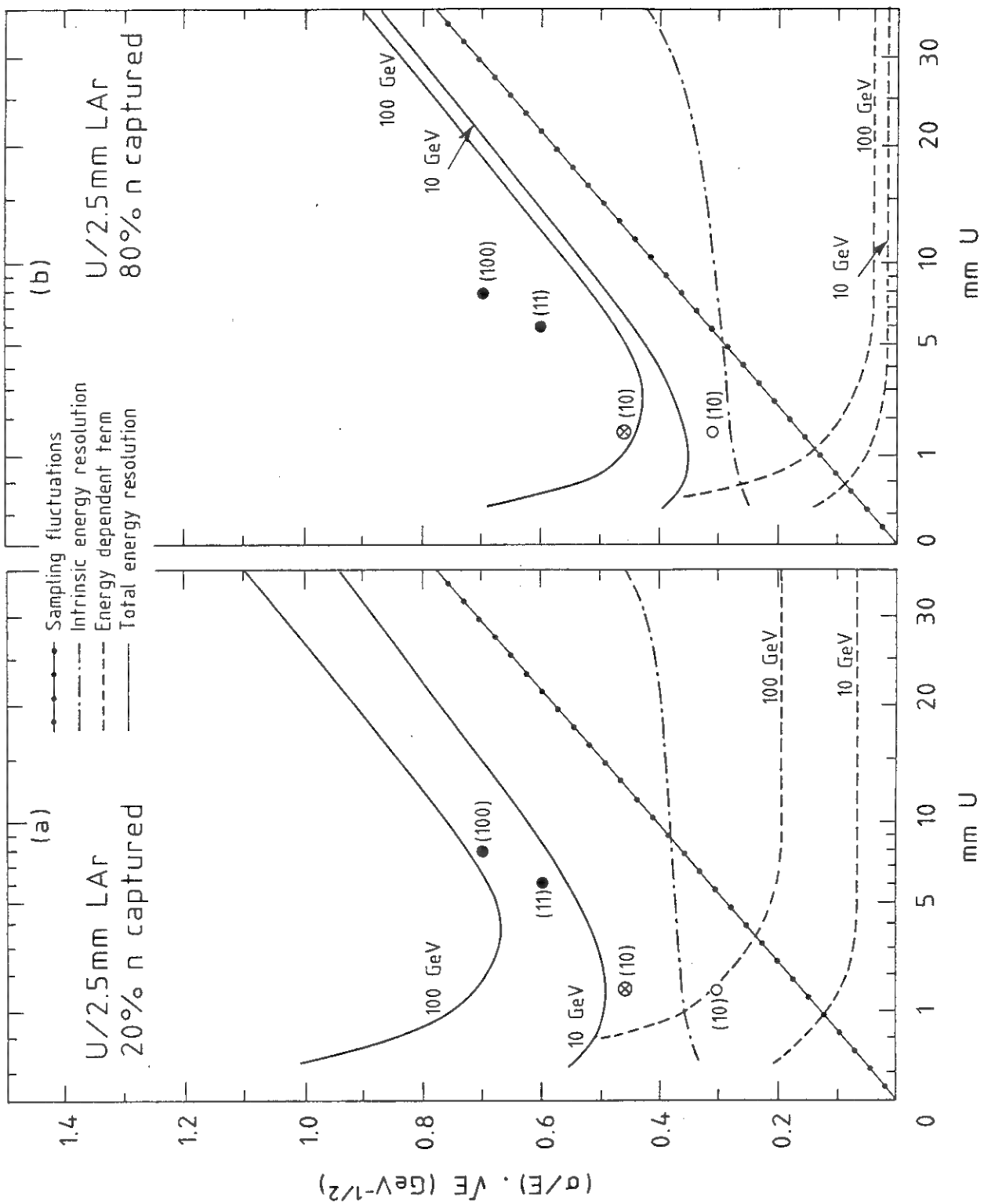
(a)
U/2.5mm LAr
20% n captured
(b)
U/2.5mm LAr
80% n captured
Sampling fluctuations
Intrinsic energy resolution
Energy dependent term
Total energy resolution
100 GeV
10 GeV
(100)
(11)
(10)
(10)
mm U
(σ/E) · √E (GeV-1/2)

Figure 18

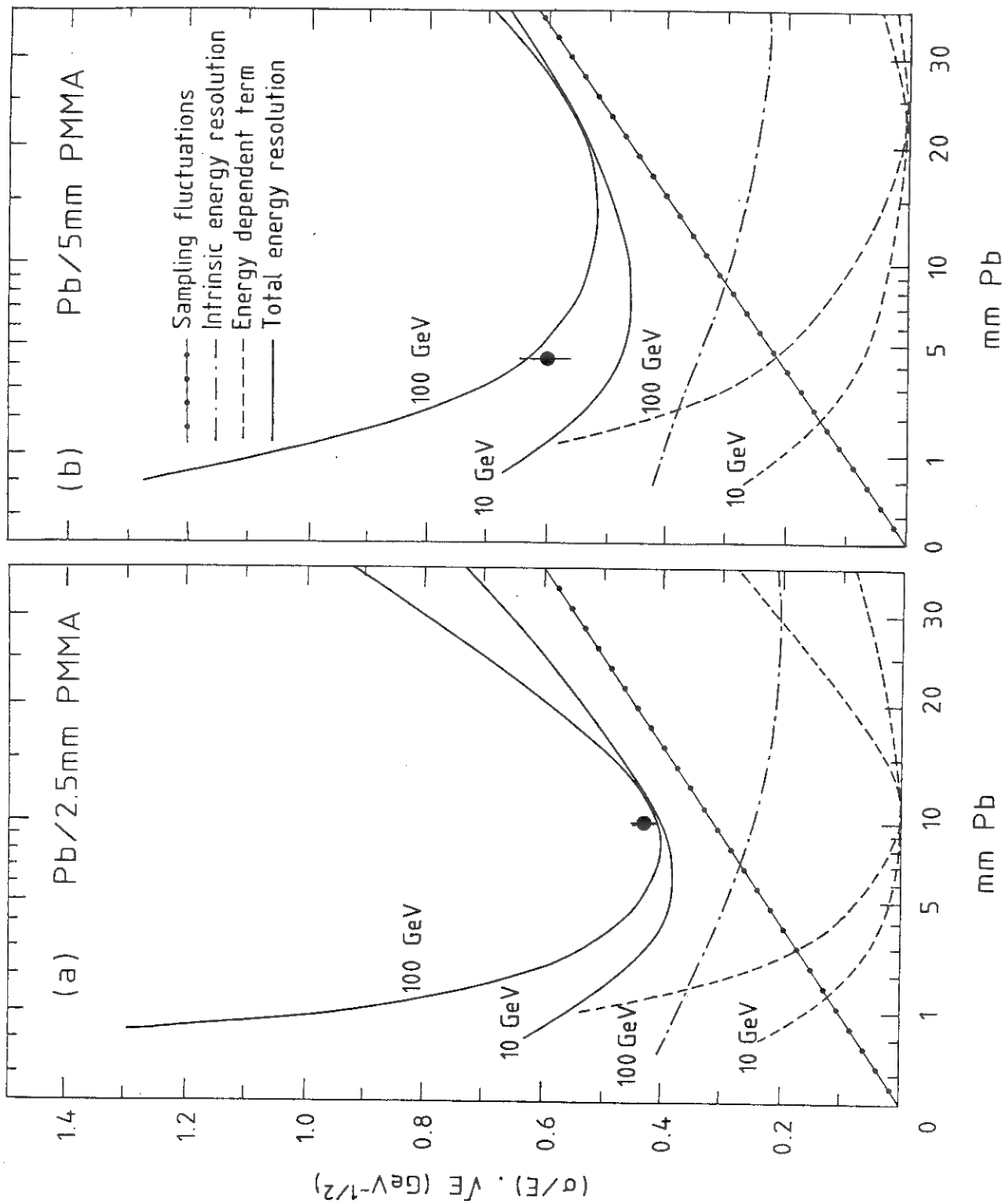
(a) Pb/2.5mm PMMA
(b) Pb/5mm PMMA
Sampling fluctuations
Intrinsic energy resolution
Energy dependent term
Total energy resolution
100 GeV
10 GeV
100 GeV
10 GeV
100 GeV
10 GeV
100 GeV
10 GeV
(σ/E) . √E (GeV-1/2)
mm Pb
mm Pb
0
0.2
0.4
0.6
0.8
1.0
1.2
1.4
1
5
10
20
30

Figure 19